HHS Public Access

Author manuscript

Hippocampus. Author manuscript; available in PMC 2024 October 01.

Published in final edited form as:

Hippocampus. 2023 October ; 33(10): 1094–1112. doi:10.1002/hipo.23567.

Structural plasticity in the entorhinal and perirhinal cortices following hippocampal lesions in rhesus monkeys

Justine Villard[1], **Loïc J. Chareyron**[1], **Olivia Piguet**[1], **Pauline Lambercy**[1], **Gianni Lonchampt**[1], **Pamela Banta Lavenex**[1,2], **David G. Amaral**[3,4], **Pierre Lavenex**[1]

[1]Laboratory of Brain and Cognitive Development, Institute of Psychology, University of Lausanne, Switzerland.

[2]Faculty of Psychology, UniDistance Suisse, Switzerland.

[3]MIND Institute and Department of Psychiatry and Behavioral Sciences, University of California at Davis.

[4]California National Primate Research Center, University of California at Davis.

Abstract

Immature neurons expressing the Bcl2 protein are present in various regions of the mammalian brain, including the amygdala and the entorhinal and perirhinal cortices. Their functional role is unknown but we have previously shown that neonatal and adult hippocampal lesions increase their differentiation in the monkey amygdala. Here, we assessed whether hippocampal lesions similarly affect immature neurons in the entorhinal and perirhinal cortices. Since Bcl2-positive cells were found mainly in areas Eo, Er and Elr of the entorhinal cortex and in layer II of the perirhinal cortex, we also used Nissl-stained sections to determine the number and soma size of immature and mature neurons in layer III of area Er and layer II of area 36 of the perirhinal cortex. We found different structural changes in these regions following hippocampal lesions, which were influenced by the time of the lesion. In neonate-lesioned monkeys, the number of immature neurons in the entorhinal and perirhinal cortices was generally higher than in controls. The number of mature neurons was also higher in layer III of area Er of neonate-lesioned monkeys but no differences were found in layer II of area 36. In adult-lesioned monkeys, the number of immature neurons in the entorhinal cortex was lower than in controls but did not differ from controls in the perirhinal cortex. The number of mature neurons in layer III of area Er did not differ from controls, but the number of small, mature neurons in layer II of area 36 was lower than in controls. In sum, hippocampal lesions impacted populations of mature and immature neurons in discrete regions and layers of the entorhinal and perirhinal cortices, which are interconnected with the amygdala and provide major cortical inputs to the hippocampus. These structural changes may contribute some functional recovery following hippocampal injury in an age-dependent manner.

*Correspondence to: Prof. Pierre Lavenex, Laboratory of Brain and Cognitive Development, Institute of Psychology, University of Lausanne, 1015 Lausanne, Switzerland, pierre.lavenex@unil.ch.

ETHICS STATEMENT

All experimental procedures were approved by the Institutional Animal Care and Use Committee of the University of California, Davis, and were in accordance with the National Institutes of Health guidelines for the use of animals in research. Research

Keywords

Medial temporal lobe; development; amnesia; memory; immature neurons; neurodevelopmental disorders

INTRODUCTION

Brain plasticity after early injury is generally considered greater than after injury occurring in adulthood (Guzzetta et al., 2010; Qi, Jain, Collins, Lyon, & Kaas, 2010; Rushmore et al., 2008; Staudt, 2010). However, the mechanisms underlying the structural brain reorganization that might enable functional recovery after early injury are poorly understood (Fiori & Guzzetta, 2015; Kolb, Gibb, & Gorny, 2000; Krageloh-Mann, Lidzba, Pavlova, Wilke, & Staudt, 2017; Thompson et al., 2009). With respect to memory and the hippocampal formation, it is well established that lesions of the hippocampus in adult humans impair both semantic and episodic memory processes (Milner, Squire, & Kandel, 1998; Verfaellie, Koseff, & Alexander, 2000). In contrast, patients who sustained hippocampal damage early in life exhibit memory impairments affecting preferentially episodic memory, whereas semantic memory is relatively preserved (Elward and Vargha-Khadem (2018) for a review). Interestingly, parallel findings were reported in monkeys with hippocampal lesion. Although hippocampal lesions prevent spatial relational learning over repeated trials in adult-lesioned monkeys (Banta Lavenex, Amaral, & Lavenex, 2006), spatial relational learning persists following neonatal lesions (Lavenex, Banta Lavenex, & Amaral, 2007). Electrophysiological and immediate early genes expression studies suggest that early hippocampal injury induces structural and functional reorganization of interconnected brain regions within the medial temporal lobe, which might compensate some of the learning and memory processes normally carried out by hippocampal circuits (Chareyron, Banta Lavenex, Amaral, & Lavenex, 2017; Duzel, Vargha-Khadem, Heinze, & Mishkin, 2001).

As a potential factor contributing to the structural and functional plasticity of the medial temporal lobe memory system following hippocampal dysfunction, populations of immature neurons expressing the anti-apoptosis Bcl2 protein have been observed in several regions of the adult mammalian brain, including the ventromedial amygdala and the temporal cortex in humans and non-human primates (Bernier, Bédard, Vinet, Lévesque, & Parent, 2002; Bernier & Parent, 1998; Fudge, 2004; Yachnis, Roper, Love, Fancey, & Muir, 2000). Primarily investigated in the amygdala, this population of Bcl2-positive immature neurons is thought to migrate from the subventricular zone (SVZ) at the tip of the ventral portion of the medial temporal horn of the lateral ventricle to the amygdala and adjoining cortex (Bernier et al., 2002). These cells are immunoreactive for other markers of neuronal immaturity, such as β-tubulin-III, PSA-NCAM and doublecortin (DCX) (Bernier et al., 2002; Chareyron, Amaral, & Lavenex, 2016; Fudge, 2004; Yachnis et al., 2000), and also express the neuronal nuclear antigen (NeuN), thus providing evidence that these cells are neurons (Chareyron et al., 2016; Sorrells et al., 2019; Yachnis et al., 2000; Zhang et al., 2009).

Although the functional role of these immature neurons remains unclear, there is evidence that they play a role in brain plasticity after hippocampal damage. Indeed, previous work from our laboratory has shown that the differentiation of immature neurons in the paralaminar nucleus of the amygdala increases following hippocampal lesions (Chareyron et al., 2016). However, different types and levels of plasticity are observed depending on the age of the animals when the lesion occurred. In adult monkeys with neonatal hippocampal lesion, the number of immature neurons in the paralaminar nucleus is higher than in control monkeys. In contrast, in monkeys with adult hippocampal lesion, the number of immature neurons in the paralaminar nucleus is lower than in control monkeys. In parallel, a higher number of mature neurons is observed in the paralaminar, basal and lateral nuclei of neonatal-lesioned monkeys, and in the paralaminar nucleus of adult-lesioned monkeys, thus suggesting that in both cases hippocampal lesions increase the differentiation of immature neurons in the amygdala. These findings further suggest that hippocampal damage or dysfunction may influence neuroblast migration from the SVZ and the differentiation of immature neurons in the amygdala (Chareyron, Banta Lavenex, Amaral, & Lavenex, 2021).

The amygdala is not the only region of the medial temporal lobe in which immature neurons are present and may differentiate following hippocampal lesions. Indeed, DCX-positive immature neurons have been reported in the monkey entorhinal and perirhinal cortices (Chareyron et al., 2021; Zhang et al., 2009), which are two prominent structures of the medial temporal lobe that play important roles in the interaction between the neocortex and the hippocampal formation in support of declarative and spatial memory functions (Lavenex & Amaral, 2000; Lavenex & Banta Lavenex, 2013; Lavenex, Suzuki, & Amaral, 2002; Morris, 2007; Piguet, Chareyron, Banta Lavenex, Amaral, & Lavenex, 2018). Here, we aimed to determine whether the immature neurons present in different subdivisions of the entorhinal and perirhinal cortices were affected by hippocampal lesions, as shown previously in the amygdala. We performed stereological analyses, using Nissl- and Bcl2-stained sections, to estimate the number and soma size of immature and mature neurons in different subdivisions of the monkey entorhinal and perirhinal cortices in the same animals used in previous studies on the amygdala (Chareyron et al., 2016; Chareyron et al., 2021). We found that most Bcl2-positive immature neurons are present in specific regions and layers of the entorhinal and perirhinal cortices, which share strong interconnections with the amygdala and relay major cortical inputs to the hippocampus. Specifically, Bcl2-positive immature neurons were found mostly in layer III of areas Eo and Er, and layer II of area Elr of the entorhinal cortex, as well as in layer II of areas 35, 36r and 36c of the perirhinal cortex. In contrast, there were very few Bcl2-positive immature neurons in the caudal subdivisions of the entorhinal cortex or in the parahippocampal cortex, thus suggesting that these immature neurons are present within very specific functional circuits of the medial temporal lobe memory system.

MATERIALS AND METHODS

Animals and lesion surgeries

Twenty-three macaque monkeys (*Macaca mulatta*) were used for this study. Monkeys were naturally born from multiparous mothers and raised at the California National Primate

Research Center (CNPRC). Experimental procedures were approved by the Institutional Animal Care and Use Committee of the University of California, Davis, and were conducted in accordance with the National Institutes of Health guidelines for the use of animals in research. To reduce the number of animals used for research, all monkeys had been involved in other studies before being included in this study (see below).

Lesion surgeries.—Bilateral hippocampal lesions were performed following the same protocol for both neonatal (12–16 days after birth) and adult (at 6.7–9.7 years of age) lesion groups (Figure 1). Detailed descriptions of these procedures can be found in (Banta Lavenex et al., 2006; Bauman, Lavenex, Mason, Capitanio, & Amaral, 2004). Briefly, all monkeys underwent presurgical magnetic resonance imaging to define the exact lesion coordinates for each individual monkey. All surgical procedures were performed aseptically at the CNPRC, with the support of veterinarians specialized in primate medicine. Monkeys were first anesthetized with ketamine hydrochloride (15 mg/kg, i.m.) and medetomidine (25–50 μg/kg, i.m.). A stable level of anesthesia was maintained throughout surgery with a combination of isoflurane (1.0%, inhalation; varied as needed to maintain an adequate level of anesthesia) and intravenous infusion of fentanyl (7–10 μg/kg/h). Monkeys were ventilated, and their vital signs were monitored throughout surgery. Simultaneous bilateral ibotenic acid (10 mg/ml in 0.1-M PBS; Biosearch Technologies, Novato, CA, USA) injections were placed into the hippocampus using 10-μl Hamilton syringes (26 gauge beveled needles) at a rate of 0.2 μl/min. Lesion extent has been described previously in Banta Lavenex et al. (2006), Lavenex et al. (2007), Chareyron et al. (2016), and Bliss-Moreau, Moadab, Santistevan, and Amaral (2017).

Unoperated control monkeys (n = 7).—The brains of four adult monkeys (5.3–9.4 years) came from previous studies of the monkey hippocampal formation (Jabès, Banta Lavenex, Amaral, & Lavenex, 2010, 2011), amygdala (Chareyron et al., 2016; Chareyron, Banta Lavenex, Amaral, & Lavenex, 2011, 2012) and entorhinal cortex (Piguet et al., 2018; Piguet, Chareyron, Banta Lavenex, Amaral, & Lavenex, 2020). These subjects were maternally reared in 2’000 m^2 outdoor enclosures and lived in large social groups until they were killed. Three additional monkeys (9.2–9.5 years) served as controls in a previous study on the plasticity of the medial temporal lobe following neonatal hippocampal lesion (Chareyron et al., 2017). They were maternally reared in 2,000 m^2 outdoor enclosures and lived in large social groups until their inclusion in the study, approximately 3 months before brain acquisition, when they were moved into indoor cages (61 cm width X 66 cm depth X 81 cm height).

Neonatal hippocampal-lesioned monkeys (n = 8).—These eight animals were part of a longitudinal study of the effects of neonatal damage to the amygdala or hippocampus on the development of social behavior (Bauman et al., 2004; Lavenex et al., 2007; Moadab, Bliss-Moreau, & Amaral, 2015) and were used in studies of the plasticity of the medial temporal lobe following hippocampal lesion (Chareyron et al., 2016; Chareyron et al., 2017). Comprehensive rearing history has been described previously (Bauman et al., 2004; Lavenex et al., 2007; Moadab et al., 2015). Briefly, infants were reared by their mothers in a socialization cohort consisting of six mother-infant pairs and one adult male. Infants were

weaned from their mothers when the youngest member of each cohort reached six months of age. Infants were then permanently housed with their previously established cohort of six infants, one adult male, and a new adult female. In addition, 2 weeks before brain acquisition, each monkey received up to five neuroanatomical tracer injections following protocols previously described (Lavenex et al., 2002; Lavenex, Suzuki, & Amaral, 2004). They were 9.1–9.4 years of age at the time their brains were collected.

The full extents of the lesions have been described in detail previously (Bliss-Moreau et al., 2017; Chareyron et al., 2016). In neonate-lesioned monkeys, the volumes of the remaining dentate gyrus granule cell layer and hippocampal fields CA3, CA2, and CA1, measured on Nissl-stained sections were, respectively, 20%, 14%, 15%, and 23% of that of controls. The volumes of the subiculum, presubiculum, and parasubiculum were, respectively, 13%, 27%, and 57% of that of controls. Portions of the parahippocampal cortex were also damaged and its average volume in neonate-lesioned monkeys was 75% of that of controls. The medial portion of cortical areas TEO and V4 sustained restricted damage in some monkeys, whereas the entorhinal and perirhinal cortices were preserved (102% and 115% of controls, respectively).

Adult hippocampal-lesioned monkeys (n = 6).—These six animals were used in studies of the role of the hippocampus in spatial learning in adult macaque monkeys (Banta Lavenex et al., 2006) and the effect of hippocampal lesion on amygdala structure (Chareyron et al., 2016). They were maternally reared in 2,000-m^2 outdoor enclosures and lived in large social groups until about one year before experimental lesion surgery (at 6–9 years of age). At that time, each monkey was moved indoors and maintained in a standard home cage. They were 10.6–13.4 years of age at the time their brains were collected.

The full extents of the lesions have been described in detail previously (Banta Lavenex et al., 2006). Briefly, the volumes of the remaining dentate gyrus granule cell layer and hippocampal fields CA3, CA2, and CA1, measured on Nissl-stained sections, were, respectively, 30%, 46%, 10%, and 14% of that of controls. The volumes of the subiculum, presubiculum, and parasubiculum were respectively 15%, 18%, and 47% of that of controls. Portions of the parahippocampal cortex were damaged and its average volume was 37% of that of controls. The entorhinal and perirhinal cortices were largely preserved (89% and 123% of that of controls, respectively). The medial portion of area TEO (from the border with area TFl to the fundus of the occipitotemporal sulcus) sustained restricted damage in some monkeys. A portion of area V4 located directly below the hippocampus was damaged in all monkeys.

Nonexperimental hippocampal-lesioned monkeys (n = 2).—Two monkeys, which participated in two previous independent studies (Banta Lavenex et al., 2006; Chareyron et al., 2017), had nonexperimental, bilateral damage to the dentate gyrus or hippocampus (Supporting Information 1; (Chareyron et al., 2016)).

The first monkey with a nonexperimental lesion of the hippocampus (NEHL1; 9.4 years) was discovered upon microscopic analysis of the brains of the control monkeys involved in a study on the functional organization of the medial temporal lobe following neonatal

hippocampal lesion (Chareyron et al., 2017). Its life history is described above and corresponds to that of the unoperated controls. NEHL1 exhibited structural abnormalities in the caudal hippocampus in both hemispheres, including granule cell dispersion in the molecular layer of the dentate gyrus, granule cell loss, and gliosis (Chareyron et al., 2016).

The second monkey with a nonexperimental lesion of the hippocampus (NEHL2; 12.6 years) was originally assigned to the control group of a study on the effect of adult hippocampus lesion on spatial relational learning (Banta Lavenex et al., 2006), and was discovered because its behavior was indistinguishable from that of experimental adult-lesioned monkeys. Its life history is described above and corresponds to that of the adult-lesioned monkeys. The extent of hippocampal damage in NEHL2 has been previously described in Banta Lavenex et al. (2006). Only the CA3, CA2, and CA1 fields of the hippocampus exhibited neuronal damage. Pyramidal neuron loss, gliosis, and cell reorganization occupied 21% of the rostrocaudal extent of the left hippocampus, and about 31% of the rostrocaudal extent of the right hippocampus.

Histological procedures

Brain acquisition.—Monkeys were deeply anesthetized with an intravenous injection of sodium pentobarbital (50 mg/kg; Fatal-Plus, Vortech Pharmaceuticals) and perfused transcardially with 1% and then 4% (wt/vol) paraformaldehyde in 0.1 M phosphate buffer (PB; pH 7.4) following standard protocols (Lavenex, Banta Lavenex, Bennett, & Amaral, 2009).

Nissl staining.—One series of 30 or 60 μm thick sections were collected in 10% (wt/vol) formaldehyde solution in 0.1 M PB (pH 7.4) and postfixed at 4 °C for 4 weeks before Nissl staining. Other series of 30 μm thick sections were collected in tissue collection solution (TCS) and kept at −70 °C until further processing. The procedure for Nissl-stained sections followed standard protocols (Lavenex et al., 2009).

NeuN, Bcl2, DCX: Neuronal phenotype markers.—We used three cell specific markers, NeuN, Bcl2, and DCX, to characterize the phenotypes of neurons in the entorhinal and perirhinal cortices. NeuN is a well-established neuron-specific marker (Mullen, Buck, & Smith, 1992). Bcl2 is an anti-apoptotic protein, which influences the rate of neuronal differentiation in young neurons and is expressed in populations of immature neurons (Bernier & Parent, 1998). DCX is a well-defined marker of immature neurons (Brown et al., 2003; Francis et al., 1999). Thirty-μm-thick sections were rinsed 3 X 10 min in 0.1 M PBS (pH 7.4) and incubated for 96 h in primary antiserum at 4 °C with gentle agitation on a rotating platform [1:50 mouse anti-Bcl2 (Abcam Cat# ab694, RRID:AB_305673) + 1:1,000 guinea-pig anti-NeuN (Merck Millipore Cat# ABN90P, RRID:AB_2341095) + 1:1,000 rabbit anti-DCX (Abcam Cat# ab18723, RRID:AB_732011) in 0.1 M PBS + 0.1% Triton X-100 + 10% (vol/vol) bovine serum (Pan Biotech, P30–0602)]. Sections were then rinsed 10 min in 0.1 M PBS, 2 X 10 min in Tris buffer, and incubated for 4 h at room temperature in secondary antiserum with gentle agitation on a rotating platform [1:400 Alexa Fluor 488-conjugated goat anti-mouse IgG (Thermo Fisher Scientific Cat# A-11029, RRID:AB_2534088) + 1:400 Alexa Fluor 568-conjugated goat anti-guinea-pig IgG (Thermo

Fisher Scientific Cat# A-11075, RRID:AB_2534119) + 1:400 Alexa Fluor 647-conjugated goat anti-rabbit IgG (Thermo Fisher Scientific Cat# A-21245, RRID:AB_2535813) in Tris buffer]. From this point on, sections were protected from light. Sections were rinsed 10 min in Tris buffer, 2 X 10 min in 0.1 M PBS, mounted on gelatin-coated slides, and air-dried overnight at room temperature. Sections were dehydrated through a graded series of ethanol solutions and coverslipped with DPX new (Merck KGaA, 100579).

Bcl2: Immature neuron marker.—We used Bcl2 immunohistochemistry to label immature neurons. One series of 30-μm-thick sections (960 μm apart) was taken from TCS and rinsed for 3 X 5 min in 0.1 M PBS containing 0.2% Triton X-100 (PBST, pH 7.4; Sigma-Aldrich, 9002–93-1), incubated for 25 min in 0.3% H_2O_2 in PBST, rinsed for 4 X 5 min in 0.1 M PBST, and incubated for 4 h in a blocking solution comprised of 3% (vol/vol) normal horse serum (Chemie Brunschwig, UP24741C) in 0.1 M PBST at room temperature. Sections were then incubated for 96 h in primary antiserum (Abcam Cat# ab694, RRID:AB_305673; at 1:50 in 0.1 M PBST) at 4 °C, rinsed for 5 X 5 min at room temperature in 0.1 M PBST, incubated for 2 h in secondary antiserum (biotinylated horse anti-mouse IgG; Vector Laboratories Cat# BA-2000, RRID:AB_2313581; at 1:250 in 0.1 M PBST), rinsed for 5 X 5 min in 0.1 M PBST, incubated for 1.5 h in avidin-biotin complex (HRP-Basic IHC kit, ImmunoBioScience, 8106) in 0.1 M PBST at room temperature, rinsed for 3 X 5 min in 0.1 M PBST, rinsed for 2 X 5 min in 0.05 M Tris buffer and incubated for 1 h in a 0.05% diaminobenzidine /0.04% H_2O_2 solution (Sigma-Aldrich, D5905). Sections were then rinsed, mounted onto gelatin-coated slides, defatted and coverslipped with DPX new.

Data acquisition and statistical analyses

Analyses of Bcl2-labeled sections.—Bcl2-positive cells (Figure 2A and B) in the entorhinal and perirhinal cortices were plotted using a 20X objective on a Nikon Eclipse 80i microscope (Nikon Instruments, Inc., Melville, NY) linked to PC-based StereoInvestigator 9.0 (MBF Bioscience, Williston, VT). Cells were counted in the right or in the left hemisphere only, as determined pseudorandomly for each animal. No differences were found between left and right hemispheres (data not shown). About nine to eleven sections per animal were used (960 μm apart) to estimate the number of Bcl2-positive cells in the entorhinal and perirhinal cortices. We used adjacent Nissl-stained sections to delineate the different subdivisions of the entorhinal and perirhinal cortices on Bcl2-stained sections. Since Bcl2-positive cells were observed in specific subdivisions and layers of these two cortices (Figure 3; see also Results section and Supporting Information 2), we also used Nissl-stained sections to analyze the number and soma size of immature and mature neurons in two of these regions: specifically, in layer III of area Er of the entorhinal cortex and in layer II of area 36 (including 36r and 36c) of the perirhinal cortex.

Stereological analyses of Nissl-stained sections.—We used the optical fractionator method on Nissl-stained sections to estimate the number of mature and immature neurons in layer III of area Er and layer II of area 36. This design-based method enables an estimation of the absolute number of neurons that is independent of the volume (Lavenex, Steele, & Jacobs, 2000). Neuron number was estimated in the right or left hemisphere, as determined

pseudorandomly for each individual. No differences were found between left and right hemispheres (data not shown). Details of the sampling schemes for different stereological counts are described in Supporting Information 3. Sampling schemes were established to obtain individual estimates of neuron number with coefficients of error (CE) around 0.10. About nine to eleven sections per animal were used for these analyses (480 μm apart for the entorhinal cortex; 960 μm apart for the perirhinal cortex), with the first section selected randomly within the first two sections through the region of interest. We used a 100X Plan Fluor oil objective (N.A. 1.30) on a Nikon Eclipse 80i microscope (Nikon Instruments, Inc., Melville, NY) linked to PC-based StereoInvestigator 2019 (MBF Bioscience, Williston, VT). The average section thickness postprocessing was 11 microns, which allowed for multiple focal planes through a 5-micron disector height and also the exclusion of partial cells with 2-micron guard zones. The volume of the soma of every neuron counted during the optical fractionator analysis was determined using the nucleator method. The nucleator is used to estimate the mean cross-sectional area and volume of cells. A set of rays emanating from a randomly chosen point within the nucleus or nucleolus is drawn and oriented randomly. The length of the intercept from the point to the cell boundary (l) is measured, and the cell volume is obtained by $V = (4/3 \times 3.1416) \times l^3$. Essentially, this is the formula used to determine the volume of a sphere with a known radius (Jabès et al., 2011). We distinguished mature and immature neurons from other cells, based on morphological criteria identifiable in Nissl preparations as previously described (Figure 2D) (Chareyron et al., 2016; Chareyron et al., 2012; García-Cabezas, John, Barbas, & Zikopoulos, 2016). Briefly, neurons are darkly stained and comprise a single large nucleolus. Immature neurons are small with round to slightly oval, hyperchromatic nuclei containing distinguishable nucleoli (Bernier et al., 2002; Fudge, 2004; Yachnis et al., 2000). The nomenclature and cytoarchitectonic organization of the monkey entorhinal and perirhinal cortices have been described in detail previously (Piguet et al., 2018; Suzuki & Amaral, 2003). We used these descriptions to delineate the different layers and subdivisions of these two cortices.

Neuronal phenotypes.—We used a confocal microscope (TCS SP5, DM6000 CFS, Leica Microsystems, Wetzlar, Germany) to determine the phenotype of immature neurons in the entorhinal and perirhinal cortices, based on the colocalization of Bcl2, NeuN, and DCX. We used a 40X objective corrected for chromatic and spherical aberration (HC PL APO 40X/1.30 oil CS2) and performed a sequential acquisition to avoid “cross-talk” between different excitation lasers and photomultiplier detection systems. Bcl2 visualization (fluorophore Alexa Fluor 488): excitation: 488 nm (argon laser); detection: 505–539 nm, gain 711, offset −1.2, pinhole 1.93 AU/126 μm. NeuN visualization (fluorophore Alexa Fluor 568): excitation: 561 nm (DPSS laser); detection: 585–624 nm, gain 805, offset 0.7, pinhole 1.93 AU/126 μm. DCX visualization (fluorophore Alexa Fluor 647): excitation: 633 nm (HeNe laser); detection: 658–688 nm, gain 728, offset 1.6, pinhole 1.93 AU/126 μm. For each acquisition, we used z-steps of 0.5 μm. We analyzed a total of 497 Bcl2+ cells (about 25 Bcl2+ cells per animal in 20 animals: 8 control, 6 neonate-lesioned and 4 adult-lesioned monkeys) using Fiji/ImageJ software v1.50b (NIH). Since there were no group differences (data not shown), the percentages of Bcl2-positive cells expressing NeuN or DCX across experimental conditions are presented in Supporting Information 4 and 5. In the entorhinal cortex, 95% of Bcl2+ cells expressed both NeuN and DCX; 0% of Bcl2+ cells expressed

NeuN but not DCX; 2% of Bcl2+ cells expressed DCX but not NeuN; and 3% of Bcl2+ cells did not express NeuN or DCX. In the perirhinal cortex, 93% of Bcl2+ cells expressed both NeuN and DCX; 0% of Bcl2+ cells expressed NeuN but not DCX; 7% of Bcl2+ cells expressed DCX but not NeuN; and 0% of Bcl2+ cells which did not express NeuN or DCX.

Statistical analyses.—We performed general linear model (GLM) analyses with the time of the lesion (neonate vs adult) as a between-subject factor on the number of immature neurons and mature neurons, as well as neuronal soma size in the entorhinal and perirhinal cortices. To compare the number of Bcl2-positive cells or Nissl-stained immature neurons between different subdivisions within the entorhinal and perirhinal cortices, we performed GLM analyses with the time of the lesion as a between-subject factor, and subdivisions of the entorhinal cortex (Eo, Er, Elr, Ei, Elc, Ec, Ecl) or perirhinal cortex (35, 36r, 36c) as repeated measures. Post hoc analyses were performed with the Fisher least significant difference test when the ANOVA *F* ratio was significant and thus controlling for type I error rate (Carmer & Swanson, 1973). Significance level was set at $p < 0.05$ for all analyses. We used the modified t-test procedure described by Crawford and Howell (1998) for the comparisons between each nonexperimentally hippocampal-lesioned monkey (NEHL1 and NEHL2) and each experimental group (control, neonatal lesion and adult lesion).

One outlier was detected in the neonate-lesioned group using the deviation around the median method (Leys, Ley, Klein, Bernard, & Licata, 2013), which is less sensitive to the presence of outliers than methods based on standard deviation and thus particularly adapted for small sample sizes. This case had a much lower number of immature neurons, which was confirmed by the analyses of both Bcl2- and Nissl-stained sections. Since we could not establish the reasons for these differences, this case was removed from all analyses (making the final number of animals in this group N = 7). Note that the results of the analyses of mature neurons did not change, whether this case was included or not.

RESULTS

Entorhinal cortex

Bcl2-positive cells.—The number of Bcl2+ cells in the entorhinal cortex differed between groups (Figure 4A; $F_{(2,17)} = 6.650$, $p = .007$, $\eta^2_p = 0.439$). Adult-lesioned monkeys had fewer Bcl2+ cells compared to neonate-lesioned ($p = .002$) and control ($p = .060$) monkeys; the difference between control and neonate-lesioned monkeys was not statistically significant ($p = .108$). Interestingly, Bcl2+ cells were mostly present in the rostral subdivisions of the entorhinal cortex (areas Eo, Er and Elr), and to a much lesser extent in the intermediate and caudal subdivisions (areas Ei, Elc, Ec, Ecl; Figure 4B). Accordingly, the number of Bcl2+ cells in the distinct subdivisions of the entorhinal cortex differed ($F_{(1.731,29.425)} = 126.038$, $p < .001$, $\eta^2_p = 0.881$; Greenhouse-Geisser correction). Moreover, group differences in the number of Bcl2+ cells varied in the distinct subdivisions (groups x subdivisions: $F_{(3.462,29.425)} = 6.968$, $p < .001$, $\eta^2_p = 0.450$). In order to make the presentation of the results more readable, the details of the statistical analyses for each subdivision are presented in Supporting Information 6. In areas Eo and Er, there were fewer Bcl2+ cells in adult-lesioned monkeys than in control and neonate-lesioned monkeys. In

contrast, in area Elr, there were more Bcl2+ cells in neonate-lesioned monkeys than in control and adult-lesioned monkeys. There were no group differences in the number of Bcl2+ cells in areas Ei, Elc, Ec and Ecl.

As can be seen in Figure 3 (see also Supporting Information 2), most Bcl2+ cells found in the entorhinal cortex were located in layer III of areas Eo and Er, and in layer II of area Elr. We therefore performed complementary analyses using Nissl-stained sections, to estimate the number and soma size of immature and mature neurons in layer III of area Er. This area was chosen considering its well defined borders and the distinct changes in the number of Bcl2+ cells when compared to layer II of the perirhinal cortex (see below).

Nissl-stained immature and mature neurons.—The number of Nissl-stained immature neurons in layer III of area Er correlated with the number of Bcl2+ cells in all layers of area Er (Supporting Information 7). The number of Nissl-stained immature neurons in layer III of area Er differed between groups (Figure 5A; $F_{(2,17)} = 8.232$, $p = .003$, $\eta^2_p = 0.492$). Neonate-lesioned monkeys had more immature neurons than control ($p = .031$) and adult-lesioned ($p < .001$) monkeys. Adult-lesioned monkeys had fewer immature neurons than control monkeys ($p = .095$). The soma size of immature neurons differed between groups (Figure 5C; $F_{(2,17)} = 8.053$, $p = .003$, $\eta^2_p = 0.487$). The average soma size of immature neurons was larger in adult-lesioned monkeys than in control ($p = .002$) and neonate-lesioned ($p = .005$) monkeys, but it did not differ between neonate-lesioned and control monkeys ($p = .572$). Furthermore, the number of small immature neurons (below the median size of controls: 120 μm^3) differed between groups (Figure 5B; $F_{(2,17)} = 12.247$, $p < .001$, $\eta^2_p = 0.590$). There were more small immature neurons in neonate-lesioned than in control ($p < .024$) and adult-lesioned ($p < .001$) monkeys; there were fewer small immature neurons in adult-lesioned than in control monkeys ($p = .024$). In contrast, the number of large immature neurons (above the median size of controls: 120 μm^3) did not differ between groups (Figure 5B; $F_{(2,17)} = 2.059$, $p = .158$, $\eta^2_p = 0.195$).

The number of mature neurons in layer III of Er differed between groups (Figure 6A; $F_{(2,17)} = 11.100$, $p < .001$, $\eta^2_p = 0.566$). Neonate-lesioned monkeys had more mature neurons than control ($p = .002$) and adult-lesioned ($p < .001$) monkeys. In contrast, the number of mature neurons did not differ between adult-lesioned and control monkeys ($p = .372$). Interestingly, similar to the results for immature neurons, the soma size of mature neurons differed between groups (Figure 6C; $F_{(2,17)} = 4.465$, $p = .028$, $\eta^2_p = 0.344$). The average soma size of mature neurons was smaller in neonate-lesioned monkeys than in control ($p = .023$) and adult-lesioned ($p = .017$) monkeys; it did not differ between adult-lesioned and control monkeys ($p = .822$). Furthermore, the number of small mature neurons (below the median size of controls: 1,800 μm^3) differed between groups (Figure 6B; $F_{(2,17)} = 13.574$, $p < .001$, $\eta^2_p = 0.615$). There was a higher number of small mature neurons in neonate-lesioned monkeys than in control ($p < .001$) and adult-lesioned ($p < .001$) monkeys; there was no difference between control and adult-lesioned monkeys ($p = .374$). In contrast, the number of large mature neurons (above the median size of controls: 1,800 μm^3) did not differ between groups (Figure 6B; $F_{(2,17)} = 2.048$, $p = .160$, $\eta^2_p = 0.194$).

Perirhinal cortex

Bcl2-positive cells.—The number of Bcl2+ cells in the perirhinal cortex differed between groups (Figure 7A; $F_{(2,17)} = 8.271$, $p = .003$, $\eta^2_p = 0.493$). Interestingly, the group differences observed in the perirhinal cortex did not correspond to what was observed in the entorhinal cortex (groups x regions: $F_{(2,17)} = 4.603$, $p = .025$, $\eta^2_p = 0.351$; see above). In the entire perirhinal cortex, there was a higher number of Bcl2+ cells in neonate-lesioned monkeys than in control ($p = .003$) and adult-lesioned ($p = .002$) monkeys, but there was no difference between adult-lesioned and control monkeys ($p = .750$). Similar to what was observed in the entorhinal cortex, however, Bcl2+ cells were more prevalent in the rostral portion of the perirhinal cortex and their distribution was largely restricted to layer II (Figure 3; Supporting Information 2). Further evidence for this rostro-caudal variability is the fact that few Bcl2+ positive cells were observed in the more caudally located parahippocampal cortex (Supporting Information 2). The number of Bcl2+ cells present in areas 35, 36r and 36c differed (Figure 7B; $F_{(1.390, 23.632)} = 102.547$, $p < .001$, $\eta^2_p = 0.858$; Greenhouse-Geisser correction). Although there was an interaction between groups and subdivisions ($F_{(2.780, 23.632)} = 3.626$, $p = .030$, $\eta^2_p = 0.299$), statistically significant group differences in the number of Bcl2+ cells were similar in areas 35, 36r and 36c (Supporting Information 6). In each subdivision of the perirhinal cortex, there were more Bcl2+ cells in neonate-lesioned monkeys than in control and adult-lesioned monkeys, and no difference between adult-lesioned and control monkeys.

Since Bcl2+ cells were mostly found in layer II of the perirhinal cortex, and since group differences did not appear to differ between areas 36r and 36c, we performed complementary analyses to estimate the number and soma size of Nissl-stained immature and mature neurons in layer II of area 36 (including areas 36r and 36c).

Nissl-stained immature and mature neurons.—The number of Nissl-stained immature neurons in layer II of area 36 correlated with the number of Bcl2+ cells in the entire perirhinal cortex (Supporting Information 7). The number of immature neurons differed between groups (Figure 8A; $F_{(2,17)} = 11.380$, $p < .001$, $\eta^2_p = 0.572$). There were more Nissl-stained immature neurons in neonate-lesioned monkeys than in control ($p = .004$) and adult-lesioned ($p < .001$) monkeys. There was no difference in the number of immature neurons between adult-lesioned and control monkeys ($p = .189$). The soma size of immature neurons differed between groups (Figure 8C; $F_{(2,17)} = 4.381$, $p = .029$, $\eta^2_p = 0.676$). The average soma size of immature neurons was larger in adult-lesioned monkeys than in control ($p = .017$) and neonate-lesioned ($p = .022$) monkeys; it did not differ between neonate-lesioned and control monkeys ($p = .899$). Furthermore, the number of small immature neurons (below the median size of controls: 130 μm^3) differed between groups (Figure 8B; $F_{(2,17)} = 11.999$, $p < .001$, $\eta^2_p = 0.585$). There were more small immature neurons in neonate-lesioned than in control ($p < .017$) and adult-lesioned ($p < .001$) monkeys; there were fewer small immature neurons in adult-lesioned than control monkeys ($p = .031$). The number of large immature neurons (above the median size of controls: 130 μm^3) did not differ between groups (Figure 8B; $F_{(2,17)} = 2.002$, $p = .166$, $\eta^2_p = 0.191$).

In contrast to what was found in layer III of area Er, there were no group differences in the number of mature neurons (Figure 9A; $F_{(2,17)} = 2.076$, $p = .156$, $\eta^2_p = 0.196$) or in their average soma size (Figure 9C; $F_{(2,17)} = 2.229$, $p = .138$, $\eta^2_p = 0.208$) in layer II of area 36. Nevertheless, there were differences between groups in the number of small neurons (below the median size of controls: 1,200 μm^3; Figure 9B; $F_{(2,17)} = 5.581$, $p = .014$, $\eta^2_p = 0.396$). There were fewer small mature neurons in adult-lesioned monkeys than in neonate-lesioned ($p = .030$) and control ($p = .005$) monkeys, but no difference between neonate-lesioned and control monkeys ($p = .363$). In contrast, there were no differences between groups in the number of large mature neurons (above the median size of controls: 1,200 μm^3; Figure 9B; $F_{(2,17)} = 0.225$, $p = .801$, $\eta^2_p = 0.026$).

Nonexperimental hippocampal lesions

The number of Bcl2+ cells in the entorhinal cortex of monkeys with a nonexperimental hippocampal lesion did not differ from control monkeys (NEHL1, $t_{(6)} = 1.885$, $p = .108$; NEHL2, $t_{(6)} = 0.776$, $p = .467$), neonate-lesioned monkeys (NEHL1, $t_{(6)} = 0.147$, $p = .888$; NEHL2, $t_{(6)} = 0.395$, $p = .707$) or adult-lesioned monkeys (NEHL1, $t_{(5)} = 1.605$, $p = .160$; NEHL2, $t_{(5)} = 1.142$, $p = .297$). In contrast, the number of Bcl2+ cells in the perirhinal cortex was higher in NEHL1 than in control monkeys ($t_{(6)} = 2.751$, $p = .033$) and adult-lesioned monkeys ($t_{(5)} = 2.326$, $p = .033$) but not neonate-lesioned monkeys ($t_{(6)} = 0.053$, $p = .959$). The number of Bcl2+ cells in the perirhinal cortex of NEHL2 did not differ from control monkeys ($t_{(6)} = 0.823$, $p = .442$), adult-lesioned monkeys ($t_{(5)} = 0.433$, $p = .680$) or neonate-lesioned monkeys ($t_{(6)} = 1.639$, $p = .152$).

Complementary analyses of Nissl-stained sections revealed no consistent differences in the number or soma size of immature and mature neurons between monkeys with a nonexperimental hippocampal lesion and control or lesioned monkeys in layer III of area Er or layer II of area 36 (Supporting Information 8-10), with the exception of a higher number of mature neurons in layer III of area Er in both NEHL cases as compared to adult-lesioned monkeys (NEHL1, $t_{(5)} = 3.053$, $p = .022$; NEHL2, $t_{(5)} = 2.237$, $p = .066$).

DISCUSSION

Here we showed that neonatal and adult hippocampal lesions are associated with distinct changes in the number of immature and mature neurons in different subdivisions of the monkey entorhinal and perirhinal cortices (see Figure 10 for a summary). In neonate-lesioned monkeys, the number of immature neurons was generally higher in the entorhinal and perirhinal cortices, as compared to both control and adult-lesioned monkeys. Moreover, the number of mature neurons was also higher in layer III of area Er of the entorhinal cortex, whereas it did not differ from controls in layer II of area 36 of the perirhinal cortex. In adult-lesioned monkeys, the number of immature neurons was lower in the entorhinal cortex as compared to controls, but it did not differ from controls in the perirhinal cortex. However, the number of small mature neurons was lower in layer II of area 36 as compared to controls, but it did not differ from controls in layer III of area Er. These results indicate that different types and levels of plasticity occur in different subdivisions of the entorhinal

and perirhinal cortices following hippocampal lesion, and that such plasticity is dependent on the age of the animal when the lesion occurred.

Neonatal hippocampal lesion

The higher number of immature neurons in the entorhinal and perirhinal cortices of neonate-lesioned monkeys may reflect increased proliferation in the SVZ and migration of neuroblasts to these cortical regions. This hypothesis is consistent with the high proliferative and migratory activity observed in the infant primate brain (Akter, Kaneko, & Sawamoto, 2021; Sanai et al., 2011), and the evidence suggesting that neuroblasts migrate from the SVZ to the temporal cortex even in adulthood (Bernier et al., 2002; Gould, Reeves, Graziano, & Gross, 1999; Shapiro, Ng, Zhou, & Ribak, 2009). However, it is also possible that immature neurons found in the entorhinal and perirhinal cortices may be generated by local precursors (Ohira et al., 2010; Tonchev, Yamashima, Sawamoto, & Okano, 2005; Xiong et al., 2010), or migrate from adjacent regions as reported in the endopirifom cortex of postnatal mice (Alderman et al., 2022).

In parallel, layer III of Er exhibited a higher number of mature neurons, particularly small neurons, in neonate-lesioned monkeys compared to both control and adult-lesioned monkeys. This suggests that some immature neurons present in layer III of Er may differentiate into small mature neurons following early hippocampal damage, which is consistent with the increased differentiation of immature neurons previously reported in the amygdala of the same monkeys (Chareyron et al., 2016). Strong evidence suggests that immature neurons in the amygdala are destined to become excitatory neurons (Sorrells et al., 2019), but it is still largely debated whether immature neurons in layer II of the cerebral cortex are destined to become principal excitatory neurons or inhibitory interneurons (Cai et al., 2009; König et al., 2016; Luzzati, Bonfanti, Fasolo, & Peretto, 2009; Varea et al., 2011; Xiong et al., 2010; Zhang et al., 2009). Although some discrepancies between studies can be attributed to technical and inter-species differences, most studies that have tried to decipher the identity and fate of immature neurons in layer II of the cerebral cortex did not necessarily focus on specific cortical regions (Coviello et al., 2022; Luzzati et al., 2009; Varea et al., 2011; Xiong et al., 2008), raising the possibility that region-specific differences exist.

In contrast, the number of mature neurons in layer II of area 36 of the perirhinal cortex did not differ from controls, suggesting that neonatal hippocampal lesion did not induce an important differentiation of immature neurons in this region, at least in layer II. Nonetheless, considering the observation of fewer small mature neurons in layer II of area 36 following adult hippocampal lesion, it remains to be determined whether some immature neurons in the perirhinal cortex of neonate-lesioned monkeys still differentiated - either in response to the lesion or naturally during development - and thus contributed to the observed stable number of small mature neurons in layer II. Interestingly, a large number of immature neurons differentiate in the primate amygdala during development (Chareyron et al., 2012; Sorrells et al., 2019). Similarly, the density of DCX-positive cells, and thus presumably immature neurons, has also been shown to decrease throughout life in layer II of the primate cerebral cortex (Srikandarajah et al., 2009; Xiong et al., 2008; Zhang et al., 2009). It is

unclear if this decrease reflects the progressive maturation or death of these immature neurons. This question will require further experimental investigation.

Adult hippocampal lesion

The lower number of immature neurons in layer III of Er and the lack of changes in layer II of area 36 in adult-lesioned monkeys support the view that the proliferation and migration of neuroblasts are more limited in adulthood than in the developing brain (Akter et al., 2021; Jabès et al., 2010; Sanai et al., 2011). Instead, the lower number of immature neurons in layer III of Er suggests that similar to what was reported for the paralaminar nucleus of the amygdala (Chareyron et al., 2016), immature neurons already present in the structure may be recruited to differentiate into mature neurons. However, contrary to what was observed in the paralaminar nucleus, the number of mature neurons in layer III of Er did not increase in adult-lesioned animals as compared to controls, thus suggesting that immature neurons may have either died or differentiated to maintain the same number of mature neurons that might have otherwise decreased following hippocampal lesion. Due to the dense interconnections between the entorhinal cortex and the hippocampus, massive adult hippocampal lesions might be expected to result in the loss of hippocampal-projecting neurons in the entorhinal cortex. However, we did not observe any change in neuron number in layer III of Er, raising the possibility that some neurons may have died and were replaced by immature neurons that differentiated.

In contrast, we observed a lower number of small mature neurons in layer II of area 36 of the perirhinal cortex following adult hippocampal lesion. This lower neuron number is unlikely to be due to inadvertant damage to the perirhinal cortex, because it was observed only for small mature neurons and not for large mature neurons, and the overall volume of the perirhinal cortex was largely preserved. Morever, no difference in the number of mature neurons was observed in neonate-lesioned monkeys with similar lesion size. One can provisionally conclude that adult hippocampal lesion was associated with the disappearance of a population of small mature neurons in layer II of area 36. Contrary to what was observed in the entorhinal cortex, in which the number of immature neurons decreased, immature neurons already present in the structure may not have been recruited - at least not more than in controls - to differentiate into mature neurons.

In sum, despite more limited proliferation and migration of neuroblasts in adulthood, adult hippocampal damage was associated with differential regulation of immature and mature neuron populations in the entorhinal and perirhinal cortices. The factors that may influence different types or levels of regulation in different structures remain to be investigated.

Nonexperimental hippocampal lesions

We found a difference in the number of Bcl2+ cells in the perirhinal cortex of case NEHL1, as compared to both control and adult-lesioned monkeys but not neonate-lesioned monkeys. In addition, we found more mature neurons in layer III of area Er for both NEHL1 and NEHL2, as compared to adult-lesioned monkeys. Interestingly, our previous data in the amygdala showed that NEHL1 had similar numbers of immature and mature neurons as neonate-lesioned monkeys, while NEHL2 followed the same trend as adult-lesioned

monkeys. The patterns observed in the entorhinal and perirhinal cortices are thus clearly different from those observed in the amygdala. Defining whether these differences are linked to different populations of immature neurons in these brain regions or differences in migration from the SVZ to these areas will require additional experimental investigation.

Functional implications

The first finding of this study is that most Bcl2-positive immature neurons are found in discrete regions and layers of the entorhinal and perirhinal cortices that share strong connections with the amygdala and relay major cortical inputs to the hippocampus (Amaral & Lavenex, 2007; Pitkanen, Kelly, & Amaral, 2002; Stefanacci, Suzuki, & Amaral, 1996; Witter, Doan, Jacobsen, Nilssen, & Ohara, 2017). More specifically, Bcl2-positive immature neurons were found mostly in layer III of areas Eo and Er, and layer II of area Elr of the entorhinal cortex, as well as in layer II of areas 35, 36r and 36c of the perirhinal cortex. In contrast, there were very few Bcl2-positive immature neurons in the caudal subdivisions of the entorhinal cortex or in the parahippocampal cortex.

Previous studies have reported that Bcl2-positive immature neurons are found in specific and interconnected regions of the primate amygdala and hippocampus (Bernier & Parent, 1998; Fudge, 2004). The current study extends this view and suggests that Bcl2-positive immature neurons are present within specific functional circuits of the medial temporal lobe memory system. Interestingly, these circuits differ in the type of information they process in support of spatial and declarative memory functions (Amaral & Lavenex, 2007; Lavenex & Amaral, 2000; Morris, 2007). The perirhinal cortex and rostral entorhinal cortex, together with the amygdala, process mainly visual object information and regulate emotional aspects of memory, while the parahippocampal cortex and caudal entorhinal cortex process mainly spatial information and contextual memory. Interestingly, Fudge, deCampo, and Becoats (2012) also found that Bcl2-positive cells in the hippocampus are particularly present in its rostral portion, a region highly connected with the amygdala (Aggleton, 1986; Fudge et al., 2012) and involved in emotional memory (Richardson, Strange, & Dolan, 2004). In addition, they reported low Bcl2 staining in the subicular complex, which, together with the caudal entorhinal cortex and parahippocampal cortex, processes spatial and contextual memory (Knierim & Neunuebel, 2016; Piguet et al., 2020; Witter & Moser, 2006). Consistent with this, Luzzati et al. (2009) observed in the guinea pig and rabbit neocortex that DCX-positive immature neurons were abundant in associative areas that are involved in non-spatial learning (but see (La Rosa et al., 2020) for phylogenetic variations in the distribution of immature neurons in the cortex). Overall, these findings raise the possibility that immature neurons or newly mature neurons may be important for the processing of non-spatial memories, such as emotional memories, and that high levels of Bcl2 protein may play a role in the functional properties of these circuits.

The second finding of this study is that important changes occur in the populations of immature and mature neurons of the entorhinal and perirhinal cortices following hippocampal lesions and that these changes are dependent on the time at which the lesion occurs. Indeed, we showed that early hippocampal damage induced a general increase in the number of immature neurons in the entorhinal and perirhinal cortices, as well as

an increase in the number of mature neurons in layer III of Er and no change in their number in layer II of area 36. In contrast, hippocampal damage in adulthood induced a decrease in the number of immature neurons in the entorhinal cortex, no change in their number in the perirhinal cortex, a decrease in the number of small mature neurons in layer II of area 36, and no change in their number in layer III of Er. These results shed light on potential mechanisms underlying the functional reorganization of the medial temporal lobe as well as the functional recovery of patients with early hippocampal damage. As mentioned previously, patients with early hippocampal damage exhibit impairments affecting preferentially episodic memory, whereas semantic memory is relatively preserved (Elward and Vargha-Khadem (2018) for a review). In contrast, patients who sustained hippocampal damage in adulthood exhibit impairements in both semantic and episodic memory processes (Milner et al., 1998; Verfaellie et al., 2000). The greater structural plasticity observed in neonate-lesioned monkeys compared to adult-lesioned monkeys is consistent with the greater functional recovery observed in patients with early hippocampal damage.

Interestingly, numerous studies reported that patients with developmental amnesia have relatively well preserved parahippocampal gyri, including the entorhinal and perirhinal cortices (Baddeley, Vargha-Khadem, & Mishkin, 2001; Bindschaedler, Peter-Favre, Maeder, Hirsbrunner, & Clarke, 2011; Brizzolara, Casalini, Montanaro, & Posteraro, 2003; Chareyron et al., 2023; Dzieciol et al., 2017; Jonin et al., 2018; Mishkin, Suzuki, Gadian, & Vargha–Khadem, 1997; Picard et al., 2013; Vargha-Khadem et al., 1997; Vicari et al., 2007). Considering that the integrity of the anterior medial temporal lobe, and particularly that of the perirhinal cortex and rostral entorhinal cortex, is essential for semantic memory function in humans (Chan et al., 2001; Davies, Graham, Xuereb, Williams, & Hodges, 2004; Galton et al., 2001), it is possible that hippocampal-lesion induced recruitement and maturation of neurons to these regions contributes to the functional preservation of semantic memory abilities observed in patients with developmental amnesia. Accordingly, a previous study from our laboratory utilizing the same neonate-lesioned monkeys as the present study found that the volume of the entorhinal and perirhinal cortices was largely preserved (Chareyron et al., 2017), with the perirhinal cortex and in particular area 36r being even larger than in controls; note that area Er of the entorhinal cortex exhibited a similar trend (unpublished data). The perirhinal cortex is particularly important for the association and discrimination of complex visual object representations, thus playing a crucial role in associative and recognition memory (Bartko, Winters, Cowell, Saksida, & Bussey, 2007; Bussey, Saksida, & Murray, 2002, 2003; Fujimichi et al., 2010; Miyashita, 2019; Naya, Yoshida, & Miyashita, 2003; Suzuki & Naya, 2014). Consistent with this hypothesis is the finding that patients with developmental amnesia exhibit good associative and recognition abilities, with some exhibiting even superior recognition for new material as compared to controls (Jonin et al., 2018), as well as excellent high-resolution binding memory performance (Allen, Atkinson, Vargha-Khadem, & Baddeley, 2022). In contrast, patients with adult-acquired hippocampal damage have impaired recognition and difficulties with high resolution binding tasks (Borders, Ranganath, & Yonelinas, 2022; Koen, Borders, Petzold, & Yonelinas, 2017).

How the lesion-induced structural changes that we present here relate to these variations in memory abilities remains to be investigated. Interestingly, the integration of new neurons in the olfactory bulb and dentate gyrus has been proposed to facilitate the distinction between overlapping memories a.k.a. pattern separation (Aimone, Wiles, & Gage, 2009; Li et al., 2018; Sahay et al., 2011), and recent evidence suggests that the perirhinal cortex interacts with the dentate gyrus to subserve memories requiring the discrimination of similar objects (Miranda et al., 2021). Whereas newly generated neurons in the dentate gyrus may have a more domain-independent role in pattern separation, it will be of great importance to investigate whether the maturation of immature neurons in the perirhinal cortex, as well as in the rostral entorhinal cortex and amygdala, may play a similar or complementary role for semantic or emotional memories.

CONCLUSION

Selective hippocampal lesions induced different changes in the number of immature and mature neurons in the entorhinal and perirhinal cortices, which were further dependent on the age of the animals when the lesion occurred. Consistent with prior findings in the amygdala, hippocampal damage may have influenced neuroblast migration and the differentiation of immature neurons in a subdivision-specific manner in the entorhinal and perirhinal cortices. Such lesion-induced neuronal plasticity may contribute to the functional reorganization of the medial temporal lobe following hippocampal damage and sheds light on potential factors that may facilitate or limit functional recovery following hippocampal injury in an age-dependent manner. Additional experimental investigations will be necessary to define the specific mechanisms that are involved.

Supplementary Material

Refer to Web version on PubMed Central for supplementary material.

ACKNOWLEDGEMENTS

We thank the CNPRC staff, Jeffrey L. Bennett, Pamela Tennant, K.C. Wells, Grégoire Favre, Jane Favre, Adeline Jabès, Hedna Scovell and Danièle Uldry for technical assistance at various stages of the project.

FUNDING INFORMATION

California National Primate Research Center, Grant/Award Number: OD011107; National Institutes of Health, Grant/Award Numbers: MH041479, NS16980, OD010962; Schweizerischer Nationalfonds zur Förderung der Wissenschaftlichen Forschung, Grant/ Award Number: P00A-106701, PP00P3-124536, and 310030_143956

DATA AVAILABILITY STATEMENT

The data that support the findings of this study are available from the corresponding author upon reasonable request.

REFERENCES

Aggleton JP (1986). A description of the amygdalo-hippocampal interconnections in the macaque monkey. Experimental Brain Research, 64(3), 515–526. doi:10.1007/bf00340489 [PubMed: 3803489]

Aimone JB, Wiles J, & Gage FH (2009). Computational influence of adult neurogenesis on memory encoding. Neuron, 61(2), 187–202. doi:10.1016/j.neuron.2008.11.026 [PubMed: 19186162]

Akter M, Kaneko N, & Sawamoto K (2021). Neurogenesis and neuronal migration in the postnatal ventricular-subventricular zone: Similarities and dissimilarities between rodents and primates. Neuroscience Research, 167, 64–69. doi:10.1016/j.neures.2020.06.001 [PubMed: 32553727]

Alderman p. J., Saxon D, Torrijos-Saiz LI, Sharief M, Biagiotti SW, Page CE, . . . Sorrells SF (2022). Mouse paralaminar amygdala excitatory neurons migrate and mature during adolescence. bioRxiv doi:10.1101/2022.09.23.509244

Allen RJ, Atkinson AL, Vargha-Khadem F, & Baddeley AD (2022). Intact high-resolution working memory binding in a patient with developmental amnesia and selective hippocampal damage. Hippocampus doi:10.1002/hipo.23452

Amaral DG, & Lavenex P (2007). Hippocampal Neuroanatomy. In Amaral DG, Andersen P, Bliss T, Morris RGM, & O'Keefe J (Eds.), The hippocampus book (Oxford University Press ed., pp. 37–114). New York: Oxford University Press.

Baddeley A, Vargha-Khadem F, & Mishkin M (2001). Preserved recognition in a case of developmental amnesia: Implications for the acquisition of semantic memory? Journal of Cognitive Neuroscience, 13(3), 357–369. doi:10.1162/08989290151137403 [PubMed: 11371313]

Banta Lavenex P, Amaral DG, & Lavenex P (2006). Hippocampal lesion prevents spatial relational learning in adult macaque monkeys. Journal of Neuroscience, 26(17), 4546–4558. doi:10.1523/JNEUROSCI.5412-05.2006. [PubMed: 16641234]

Bartko SJ, Winters BD, Cowell RA, Saksida LM, & Bussey TJ (2007). Perirhinal cortex resolves feature ambiguity in configural object recognition and perceptual oddity tasks. Learning & Memory, 14(12), 821–832. doi:10.1101/lm.749207 [PubMed: 18086825]

Bauman MD, Lavenex P, Mason WA, Capitanio JP, & Amaral DG (2004). The development of social behavior following neonatal amygdala lesions in rhesus monkeys. Journal of Cognitive Neuroscience, 16(8), 1388–1411. doi:10.1162/0898929042304741 [PubMed: 15509386]

Bernier PJ, Bédard A, Vinet J, Lévesque M, & Parent A (2002). Newly generated neurons in the amygdala and adjoining cortex of adult primates. Proceedings of the National Academy of Sciences, 99(17), 11464–11469. doi:10.1073/pnas.172403999

Bernier PJ, & Parent A (1998). Bcl-2 protein as a marker of neuronal immaturity in postnatal primate brain. Journal of Neuroscience, 18(7), 2486–2497. doi:10.1523/jneurosci.18-07-02486.1998 [PubMed: 9502809]

Bindschaedler C, Peter-Favre C, Maeder P, Hirsbrunner T, & Clarke S (2011). Growing up with bilateral hippocampal atrophy: From childhood to teenage. Cortex, 47(8), 931–944. doi:10.1016/j.cortex.2010.09.005 [PubMed: 21055737]

Bliss-Moreau E, Moadab G, Santistevan A, & Amaral DG (2017). The effects of neonatal amygdala or hippocampus lesions on adult social behavior. Behav Brain Res, 322(Pt A), 123–137. doi:10.1016/j.bbr.2016.11.052 [PubMed: 28017854]

Borders AA, Ranganath C, & Yonelinas AP (2022). The hippocampus supports high-precision binding in visual working memory. Hippocampus, 32(3), 217–230. doi:10.1002/hipo.23401 [PubMed: 34957640]

Brizzolara D, Casalini C, Montanaro D, & Posteraro F (2003). A case of amnesia at an early age. Cortex, 39(4–5), 605–625. doi:10.1016/S0010-9452(08)70856-6 [PubMed: 14584545]

Brown JP, Couillard-Despres S, Cooper-Kuhn CM, Winkler J, Aigner L, & Kuhn HG (2003). Transient expression of doublecortin during adult neurogenesis. Journal of Comparative Neurology, 467(1), 1–10. doi:10.1002/cne.10874 [PubMed: 14574675]

Bussey TJ, Saksida LM, & Murray EA (2002). Perirhinal cortex resolves feature ambiguity in complex visual discriminations. European Journal of Neuroscience, 15(2), 365–374. doi:10.1046/j.0953-816x.2001.01851.x [PubMed: 11849302]

Bussey TJ, Saksida LM, & Murray EA (2003). Impairments in visual discrimination after perirhinal cortex lesions: testing 'declarative' vs. 'perceptual-mnemonic' views of perirhinal cortex function. European Journal of Neuroscience, 17(3), 649–660. doi:10.1046/j.1460-9568.2003.02475.x [PubMed: 12581183]

Cai Y, Xiong K, Chu Y, Luo D-W, Luo X-G, Yuan X-Y, . . . Yan X-X (2009). Doublecortin expression in adult cat and primate cerebral cortex relates to immature neurons that develop into GABAergic subgroups. Experimental Neurology, 216(2), 342–356. doi:10.1016/j.expneurol.2008.12.008 [PubMed: 19166833]

Chan D, Fox NC, Scahill RI, Crum WR, Whitwell JL, Leschziner G, . . . Rossor MN (2001). Patterns of temporal lobe atrophy in semantic dementia and Alzheimer's disease. Annals of Neurology, 49(4), 433–442. doi:10.1002/ana.92 [PubMed: 11310620]

Chareyron LJ, Amaral DG, & Lavenex P (2016). Selective lesion of the hippocampus increases the differentiation of immature neurons in the monkey amygdala. Proceedings of the National Academy of Sciences, 113(50), 14420–14425. doi:10.1073/pnas.1604288113

Chareyron LJ, Banta Lavenex P, Amaral DG, & Lavenex P (2011). Stereological analysis of the rat and monkey amygdala. Journal of Comparative Neurology, 519(16), 3218–3239. doi:10.1002/cne.22677 [PubMed: 21618234]

Chareyron LJ, Banta Lavenex P, Amaral DG, & Lavenex P (2012). Postnatal development of the amygdala: A stereological study in macaque monkeys. Journal of Comparative Neurology, 520(9), 1965–1984. doi:10.1002/cne.23023 [PubMed: 22173686]

Chareyron LJ, Banta Lavenex P, Amaral DG, & Lavenex P (2017). Functional organization of the medial temporal lobe memory system following neonatal hippocampal lesion in rhesus monkeys. Brain Structure and Function, 222(9), 3899–3914. doi:10.1007/s00429-017-1441-z [PubMed: 28488186]

Chareyron LJ, Banta Lavenex P, Amaral DG, & Lavenex P (2021). Life and death of immature neurons in the juvenile and adult primate amygdala. International Journal of Molecular Sciences, 22(13). doi:10.3390/ijms22136691

Chareyron LJ, Chong K, Banks T, Mishkin M, Burgesse N, Saunders RC, & Vargha-Khadem F (2023). Paradoxical consequences of early hippocampal damage: Greater atrophy is associated with better recall, working memory and visuospatial perception in developmental amnesia. bioRxiv doi:10.1101/2023.01.23.525152

Coviello S, Gramuntell Y, Klimczak P, Varea E, Blasco-Ibanez JM, Crespo C, . . . Nacher J (2022). Phenotype and distribution of immature neurons in the human cerebral cortex layer II. Front Neuroanat, 16, 851432. doi:10.3389/fnana.2022.851432 [PubMed: 35464133]

Davies RR, Graham KS, Xuereb JH, Williams GB, & Hodges JR (2004). The human perirhinal cortex and semantic memory. European Journal of Neuroscience, 20(9), 2441–2446. doi:10.1111/j.1460-9568.2004.03710.x [PubMed: 15525284]

Duzel E, Vargha-Khadem F, Heinze HJ, & Mishkin M (2001). Brain activity evidence for recognition without recollection after early hippocampal damage. Proceedings of the National Academy of Sciences, 98(14), 8101–8106. doi:10.1073/pnas.131205798

Dzieciol AM, Bachevalier J, Saleem KS, Gadian DG, Saunders R, Chong WKK, . . . Vargha-Khadem F (2017). Hippocampal and diencephalic pathology in developmental amnesia. Cortex, 86, 33–44. doi:10.1016/j.cortex.2016.09.016 [PubMed: 27880886]

Elward RL, & Vargha-Khadem F (2018). Semantic memory in developmental amnesia. Neuroscience Letters, 680, 23–30. doi:10.1016/j.neulet.2018.04.040 [PubMed: 29715544]

Fiori S, & Guzzetta A (2015). Plasticity following early-life brain injury: Insights from quantitative MRI. Seminars in Perinatology, 39(2), 141–146. doi:10.1053/j.semperi.2015.01.007 [PubMed: 25813668]

Francis F, Koulakoff A, Boucher D, Chafey P, Schaar B, Vinet M-C, . . . Chelly J (1999). Doublecortin is a developmentally regulated, microtubule-associated protein expressed in migrating and differentiating neurons. Neuron, 23(2), 247–256. doi:10.1016/s0896-6273(00)80777-1 [PubMed: 10399932]

Fudge JL (2004). Bcl-2 immunoreactive neurons are differentially distributed in subregions of the amygdala and hippocampus of the adult macaque. Neuroscience, 127(2), 539–556. doi:10.1016/j.neuroscience.2004.05.019 [PubMed: 15262342]

Fudge JL, deCampo DM, & Becoats KT (2012). Revisiting the hippocampal–amygdala pathway in primates: Association with immature-appearing neurons. Neuroscience, 212, 104–119. doi:10.1016/j.neuroscience.2012.03.040 [PubMed: 22521814]

Fujimichi R, Naya Y, Koyano KW, Takeda M, Takeuchi D, & Miyashita Y (2010). Unitized representation of paired objects in area 35 of the macaque perirhinal cortex. European Journal of Neuroscience, 32(4), 659–667. doi:10.1111/j.1460-9568.2010.07320.x [PubMed: 20718858]

Galton CJ, Patterson K, Graham K, Lambon-Ralph MA, Williams G, Antoun N, . . . Hodges JR (2001). Differing patterns of temporal atrophy in Alzheimer's disease and semantic dementia. Neurology, 57(2), 216–225. doi:10.1212/wnl.57.2.216 [PubMed: 11468305]

García-Cabezas MÁ, John YJ, Barbas H, & Zikopoulos B (2016). Distinction of neurons, glia and endothelial cells in the cerebral cortex: An algorithm based on cytological features. Frontiers in Neuroanatomy, 10. doi:10.3389/fnana.2016.00107

Gould E, Reeves AJ, Graziano MSA, & Gross CG (1999). Neurogenesis in the neocortex of adult primates. Science, 286(5439), 548–552. doi:10.1126/science.286.5439.548 [PubMed: 10521353]

Guzzetta A, D'Acunto G, Rose S, Tinelli F, Boyd R, & Cioni G (2010). Plasticity of the visual system after early brain damage. Developmental Medicine & Child Neurology doi:10.1111/j.1469-8749.2010.03710.x

Jabès A, Banta Lavenex P, Amaral DG, & Lavenex P (2010). Quantitative analysis of postnatal neurogenesis and neuron number in the macaque monkey dentate gyrus. European Journal of Neuroscience, 31(2), 273–285. doi:10.1111/j.1460-9568.2009.07061.x [PubMed: 20074220]

Jabès A, Banta Lavenex P, Amaral DG, & Lavenex P (2011). Postnatal development of the hippocampal formation: A stereological study in macaque monkeys. Journal of Comparative Neurology, 519(6), 1051–1070. doi:10.1002/cne.22549 [PubMed: 21344402]

Jonin PY, Besson G, La Joie R, Pariente J, Belliard S, Barillot C, & Barbeau EJ (2018). Superior explicit memory despite severe developmental amnesia: In-depth case study and neural correlates. Hippocampus, 28(12), 867–885. doi:10.1002/hipo.23010 [PubMed: 29995351]

Knierim JJ, & Neunuebel JP (2016). Tracking the flow of hippocampal computation: Pattern separation, pattern completion, and attractor dynamics. Neurobiology of Learning and Memory, 129, 38–49. doi:10.1016/j.nlm.2015.10.008 [PubMed: 26514299]

Koen JD, Borders AA, Petzold MT, & Yonelinas AP (2017). Visual short-term memory for high resolution associations is impaired in patients with medial temporal lobe damage. Hippocampus, 27(2), 184–193. doi:10.1002/hipo.22682 [PubMed: 27859914]

Kolb B, Gibb R, & Gorny G (2000). Cortical plasticity and the development of behavior after early frontal cortical injury. Developmental Neuropsychology, 18(3), 423–444. doi:10.1207/S1532694208Kolb [PubMed: 11385833]

König R, Benedetti B, Rotheneichner P, O'Sullivan A, Kreutzer M, Belles M, . . . Couillard-Despres S (2016). Distribution and fate of DCX/PSA-NCAM expressing cells in the adult mammalian cortex: A local reservoir for adult cortical neuroplasticity? Frontiers in Biology, 11, 193–216. doi:10.1007/s11515-016-1403-5

Krageloh-Mann I, Lidzba K, Pavlova MA, Wilke M, & Staudt M (2017). Plasticity during early brain development is determined by ontogenetic potential. Neuropediatrics, 48(2), 66–71. doi:10.1055/s-0037-1599234 [PubMed: 28282668]

La Rosa C, Cavallo F, Pecora A, Chincarini M, Ala U, Faulkes CG, . . . Bonfanti L (2020). Phylogenetic variation in cortical layer II immature neuron reservoir of mammals. eLife, 9. doi:10.7554/eLife.55456

Lavenex P, & Amaral DG (2000). Hippocampal-neocortical interaction: A hierarchy of associativity. Hippocampus, 10(4), 420–430. doi:10.1002/1098-1063(2000)10:4<420::AID-HIPO8>3.0.CO;2-5 [PubMed: 10985281]

Lavenex P, & Banta Lavenex P (2013). Building hippocampal circuits to learn and remember: Insights into the development of human memory. Behavioural Brain Research, 254, 8–21. doi:10.1016/j.bbr.2013.02.007 [PubMed: 23428745]

Lavenex P, Banta Lavenex P, & Amaral DG (2007). Spatial relational learning persists following neonatal hippocampal lesions in macaque monkeys. Nature Neuroscience, 10(2), 234–239. doi:10.1038/nn1820 [PubMed: 17195843]

Lavenex P, Banta Lavenex P, Bennett JL, & Amaral DG (2009). Postmortem changes in the neuroanatomical characteristics of the primate brain: The hippocampal formation. Journal of Comparative Neurology, 512(1), 27–51. doi:10.1002/cne.21906 [PubMed: 18972553]

Lavenex P, Steele MA, & Jacobs LF (2000). Sex differences, but no seasonal variations in the hippocampus of food-caching squirrels: a stereological study. J Comp Neurol, 425(1), 152–166. Retrieved from https://www.ncbi.nlm.nih.gov/pubmed/10940949 [PubMed: 10940949]

Lavenex P, Suzuki WA, & Amaral DG (2002). Perirhinal and parahippocampal cortices of the macaque monkey: Projections to the neocortex. Journal of Comparative Neurology, 447(4), 394–420. doi:10.1002/cne.10243 [PubMed: 11992524]

Lavenex P, Suzuki WA, & Amaral DG (2004). Perirhinal and parahippocampal cortices of the macaque monkey: Intrinsic projections and interconnections. Journal of Comparative Neurology, 472(3), 371–394. doi:10.1002/cne.20079 [PubMed: 15065131]

Leys C, Ley C, Klein O, Bernard P, & Licata L (2013). Detecting outliers: Do not use standard deviation around the mean, use absolute deviation around the median. Journal of Experimental Social Psychology, 49(4), 764–766. doi:10.1016/j.jesp.2013.03.013

Li WL, Chu MW, Wu A, Suzuki Y, Imayoshi I, & Komiyama T (2018). Adult-born neurons facilitate olfactory bulb pattern separation during task engagement. eLife, 7. doi:10.7554/elife.33006

Luzzati F, Bonfanti L, Fasolo A, & Peretto P (2009). DCX and PSA-NCAM expression identifies a population of neurons preferentially distributed in associative areas of different pallial derivatives and vertebrate species. Cerebral Cortex, 19(5), 1028–1041. doi:10.1093/cercor/bhn145 [PubMed: 18832334]

Milner B, Squire LR, & Kandel ER (1998). Cognitive neuroscience and the study of memory. Neuron, 20(3), 445–468. doi:10.1016/s0896-6273(00)80987-3 [PubMed: 9539121]

Miranda M, Morici JF, Gallo F, Piromalli Girado D, Weisstaub NV, & Bekinschtein P (2021). Molecular mechanisms within the dentate gyrus and the perirhinal cortex interact during discrimination of similar nonspatial memories. Hippocampus, 31(2), 140–155. doi:10.1002/hipo.23269 [PubMed: 33064924]

Mishkin M, Suzuki WA, Gadian DG, & Vargha–Khadem F (1997). Hierarchical organization of cognitive memory. Philosophical Transactions of the Royal Society of London. Series B: Biological Sciences, 352(1360), 1461–1467. doi:10.1098/rstb.1997.0132 [PubMed: 9368934]

Miyashita Y (2019). Perirhinal circuits for memory processing. Nature Reviews Neuroscience, 20(10), 577–592. doi:10.1038/s41583-019-0213-6 [PubMed: 31485007]

Moadab G, Bliss-Moreau E, & Amaral DG (2015). Adult social behavior with familiar partners following neonatal amygdala or hippocampus damage. Behavioral Neuroscience, 129(3), 339–350. doi:10.1037/bne0000062 [PubMed: 26030432]

Morris RGM (2007). Theories of hippocampal function. In Amaral DG, Andersen P, Bliss T, Morris RGM, & O'Keefe J (Eds.), The hippocampus book (Oxford University Press ed., pp. 581–714). New York: Oxford University Press.

Mullen RJ, Buck CR, & Smith AM (1992). NeuN, a neuronal specific nuclear protein in vertebrates. Development, 116(1), 201–211. doi:10.1242/dev.116.1.201 [PubMed: 1483388]

Naya Y, Yoshida M, & Miyashita Y (2003). Forward processing of long-term associative memory in monkey inferotemporal cortex. Journal of Neuroscience, 23(7), 2861–2871. doi:10.1523/JNEUROSCI.23-07-02861.2003 [PubMed: 12684473]

Ohira K, Furuta T, Hioki H, Nakamura KC, Kuramoto E, Tanaka Y, . . . Nakamura S (2010). Ischemia-induced neurogenesis of neocortical layer 1 progenitor cells. Nature Neuroscience, 13(2), 173–179. doi:10.1038/nn.2473 [PubMed: 20037576]

Picard L, Mayor-Dubois C, Maeder P, Kalenzaga S, Abram M, Duval C, . . . Piolino P (2013). Functional independence within the self-memory system: New insights from two cases of developmental amnesia. Cortex, 49(6), 1463–1481. doi:10.1016/j.cortex.2012.10.003 [PubMed: 23261550]

Piguet O, Chareyron LJ, Banta Lavenex P, Amaral DG, & Lavenex P (2018). Stereological analysis of the rhesus monkey entorhinal cortex. Journal of Comparative Neurology, 526(13), 2115–2132. doi:10.1002/cne.24496 [PubMed: 30004581]

Piguet O, Chareyron LJ, Banta Lavenex P, Amaral DG, & Lavenex P (2020). Postnatal development of the entorhinal cortex: A stereological study in macaque monkeys. Journal of Comparative Neurology. doi:10.1002/cne.24897

Pitkanen A, Kelly JL, & Amaral DG (2002). Projections from the lateral, basal, and accessory basal nuclei of the amygdala to the entorhinal cortex in the macaque monkey. Hippocampus, 12(2), 186–205. doi:10.1002/hipo.1099 [PubMed: 12000118]

Qi HX, Jain N, Collins CE, Lyon DC, & Kaas JH (2010). Functional organization of motor cortex of adult macaque monkeys is altered by sensory loss in infancy. Proceedings of the National Academy of Sciences, 107(7), 3192–3197. doi:10.1073/pnas.0914962107.

Richardson MP, Strange BA, & Dolan RJ (2004). Encoding of emotional memories depends on amygdala and hippocampus and their interactions. Nature Neuroscience, 7(3), 278–285. doi:10.1038/nn1190 [PubMed: 14758364]

Rushmore RJ, Rigolo L, Peer AK, Afifi LM, Valero-Cabre A, & Payne BR (2008). Age-dependent sparing of visual function after bilateral lesions of primary visual cortex. Behavioral Neuroscience, 122(6), 1274–1283. doi:10.1037/a0013586. [PubMed: 19045947]

Sahay A, Scobie KN, Hill AS, O'Carroll CM, Kheirbek MA, Burghardt NS, . . . Hen R (2011). Increasing adult hippocampal neurogenesis is sufficient to improve pattern separation. Nature, 472(7344), 466–470. doi:10.1038/nature09817 [PubMed: 21460835]

Sanai N, Nguyen T, Ihrie RA, Mirzadeh Z, Tsai H-H, Wong M, . . . Alvarez-Buylla A (2011). Corridors of migrating neurons in the human brain and their decline during infancy. Nature, 478(7369), 382–386. doi:10.1038/nature10487 [PubMed: 21964341]

Shapiro LA, Ng K, Zhou Q-Y, & Ribak CE (2009). Subventricular zone-derived, newly generated neurons populate several olfactory and limbic forebrain regions. Epilepsy & Behavior, 14(1), 74–80. doi:10.1016/j.yebeh.2008.09.011 [PubMed: 18849007]

Sorrells SF, Paredes MF, Velmeshev D, Herranz-Pérez V, Sandoval K, Mayer S, . . . Alvarez-Buylla A (2019). Immature excitatory neurons develop during adolescence in the human amygdala. Nature Communications, 10(1). doi:10.1038/s41467-019-10765-1

Srikandarajah N, Martinian L, Sisodiya SM, Squier W, Blumcke I, Aronica E, & Thom M (2009). Doublecortin expression in focal cortical dysplasia in epilepsy. Epilepsia, 50(12), 2619–2628. doi:10.1111/j.1528-1167.2009.02194.x [PubMed: 19583780]

Staudt M (2010). Reorganization after pre- and perinatal brain lesions*. Journal of Anatomy. doi:10.1111/j.1469-7580.2010.01262.x

Stefanacci L, Suzuki WA, & Amaral DG (1996). Organization of connections between the amygdaloid complex and the perirhinal and parahippocampal cortices in macaque monkeys. Journal of Comparative Neurology, 375(4), 552–582. doi:10.1002/(SICI)1096-9861(19961125)375:4<552::AID-CNE2>3.0.CO;2-0 [PubMed: 8930786]

Suzuki WA, & Amaral DG (2003). Perirhinal and parahippocampal cortices of the macaque monkey: Cytoarchitectonic and chemoarchitectonic organization. Journal of Comparative Neurology, 463(1), 67–91. doi:10.1002/cne.10744 [PubMed: 12811804]

Suzuki WA, & Naya Y (2014). The Perirhinal Cortex. Annual Review of Neuroscience, 37(1), 39–53. doi:10.1146/annurev-neuro-071013-014207

Thompson K, Biddle KR, Robinson-Long M, Poger J, Wang J, Yang QX, & Eslinger PJ (2009). Cerebral plasticity and recovery of function after childhood prefrontal cortex damage. Developmental Neurorehabilitation, 12(5), 298–312. doi:10.3109/17518420903236262 [PubMed: 20477559]

Tonchev AB, Yamashima T, Sawamoto K, & Okano H (2005). Enhanced proliferation of progenitor cells in the subventricular zone and limited neuronal production in the striatum and neocortex of adult macaque monkeys after global cerebral ischemia. Journal of Neuroscience Research, 81(6), 776–788. doi:10.1002/jnr.20604 [PubMed: 16047371]

Varea E, Belles M, Vidueira S, Blasco-Ibanez JM, Crespo C, Pastor AM, & Nacher J (2011). PSA-NCAM is expressed in immature, but not recently generated, neurons in the adult cat cerebral cortex layer II. Frontiers in Neuroscience, 5, 17. doi:10.3389/fnins.2011.00017 [PubMed: 21415912]

Vargha-Khadem F, Gadian DG, Watkins KE, Connelly A, Van Paesschen W, & Mishkin M (1997). Differential effects of early hippocampal pathology on episodic and semantic memory. Science, 277(5324), 376–380. doi:10.1126/science.277.5324.376 [PubMed: 9219696]

Verfaellie M, Koseff P, & Alexander MP (2000). Acquisition of novel semantic information in amnesia: effects of lesion location. Neuropsychologia, 38(4), 484–492. doi:10.1016/s0028-3932(99)00089-5 [PubMed: 10683398]

Vicari S, Menghini D, Di Paola M, Serra L, Donfrancesco A, Fidani P, . . . Carlesimo GA (2007). Acquired amnesia in childhood: A single case study. Neuropsychologia, 45(4), 704–715. doi:10.1016/j.neuropsychologia.2006.08.004 [PubMed: 16989873]

Witter MP, Doan TP, Jacobsen B, Nilssen ES, & Ohara S (2017). Architecture of the entorhinal cortex a review of entorhinal anatomy in rodents with some comparative notes. Frontiers in Systems Neuroscience, 11. doi:10.3389/fnsys.2017.00046

Witter MP, & Moser EI (2006). Spatial representation and the architecture of the entorhinal cortex. Trends in Neurosciences, 29(12), 671–678. doi:10.1016/j.tins.2006.10.003 [PubMed: 17069897]

Xiong K, Cai Y, Zhang X-M, Huang J-F, Liu Z-Y, Fu G-M, . . . Yan X-X (2010). Layer I as a putative neurogenic niche in young adult guinea pig cerebrum. Molecular and Cellular Neuroscience, 45(2), 180–191. doi:10.1016/j.mcn.2010.06.009 [PubMed: 20599617]

Xiong K, Luo D-W, Patrylo PR, Luo X-G, Struble RG, Clough RW, & Yan X-X (2008). Doublecortin-expressing cells are present in layer II across the adult guinea pig cerebral cortex: Partial colocalization with mature interneuron markers. Experimental Neurology, 211(1), 271–282. doi:10.1016/j.expneurol.2008.02.003 [PubMed: 18378231]

Yachnis AT, Roper SN, Love A, Fancey JT, & Muir D (2000). Bcl-2 immunoreactive cells with immature neuronal phenotype exist in the nonepileptic adult human brain. Journal of Neuropathology & Experimental Neurology, 59(2), 113–119. doi:10.1093/jnen/59.2.113 [PubMed: 10749100]

Zhang XM, Cai Y, Chu Y, Chen EY, Feng JC, Luo XG, . . . Yan XX (2009). Doublecortin-expressing cells persist in the associative cerebral cortex and amygdala in aged nonhuman primates. Frontiers in Neuroanatomy, 3, 17. doi:10.3389/neuro.05.017.2009 [PubMed: 19862344]

Figure 1.

Nissl-stained sections of the monkey medial temporal lobe at mid rostrocaudal level of the hippocampus showing the hippocampal formation in the three experimental groups. **A.** Adult, unoperated control monkey. **B.** Adult monkey with neonatal hippocampal lesion. **C.** Adult monkey with adult hippocampal lesion. (Scale bar for all three panels, 2 mm.) Reproduced with permission from (Chareyron et al., 2016).

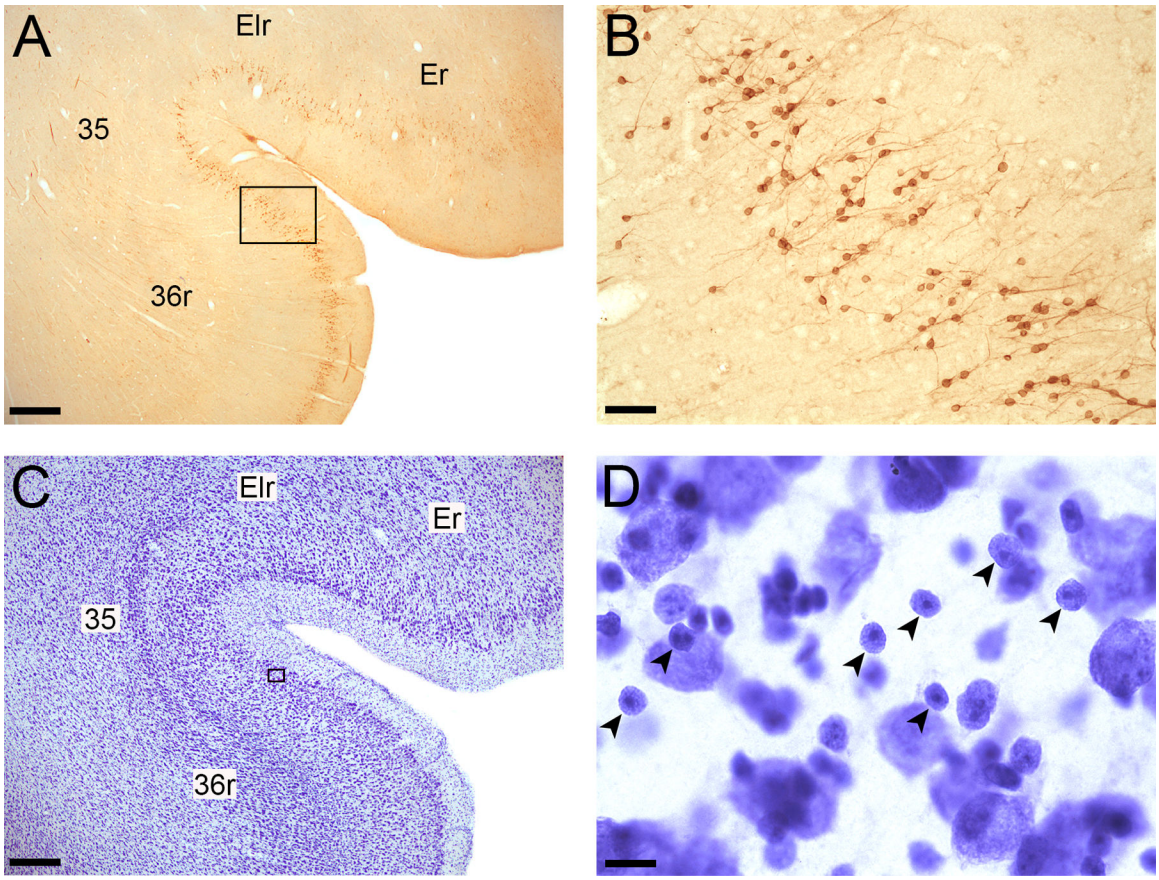

Figure 2.

Examples of Bcl2 and Nissl-stained immature neurons in the perirhinal cortex. **A**. Bcl2-stained section showing areas Er and Elr of the entorhinal cortex and areas 35 and 36r of the perirhinal cortex; Magnification: 2X; Scale bar: 500 μm. **B.** Bcl2+ cells and thin processes visible within layer II of the perirhinal cortex; 20X; Scale bar: 50 μm. **C.** Nissl-stained section showing areas Er and Elr of the entorhinal cortex and areas 35 and 36r of the perirhinal cortex; 2X; Scale bar: 500 μm **B.** Nissl-stained immature neurons (small arrowheads) within layer II of the perirhinal cortex; 100X; Scale bar: 10 μm.

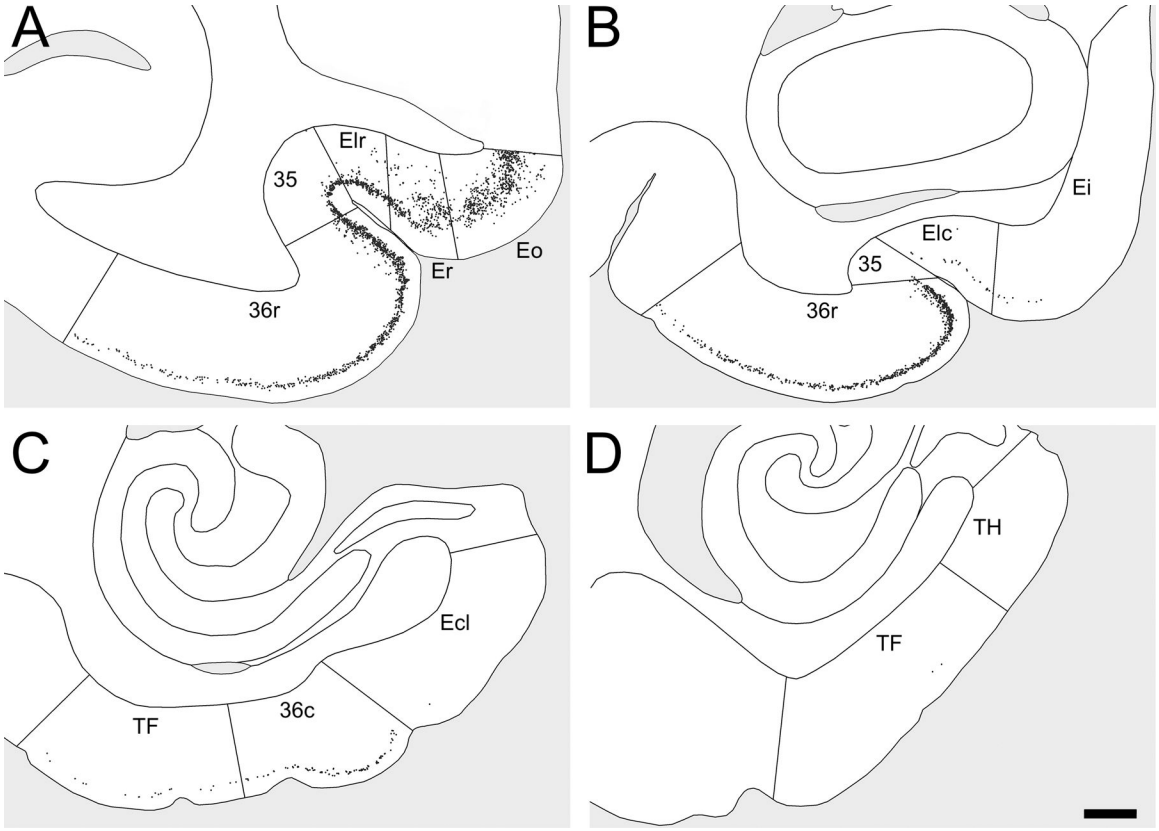

Figure 3.

Distribution of Bcl2+ cells in the distinct subdivisions of the entorhinal, perirhinal and parahippocampal cortices of a control monkey. Note that Bcl2+ cells in adjacent brain regions are not represented. **A.** Bcl2+ cells in areas Eo, Er and Elr of the entorhinal cortex and in areas 35 and 36r of the perirhinal cortex. **B.** Bcl2+ cells in areas Ei and Elc of the entorhinal cortex and in areas 35 and 36r of the perirhinal cortex. **C.** Bcl2+ cells in area Ecl of the entorhinal cortex, area 36c of the perirhinal cortex and area TF of the parahippocampal cortex. **D.** Bcl2+ cells in areas TF and TH of the parahippocampal cortex. Scale bar for all panels, 1 mm.

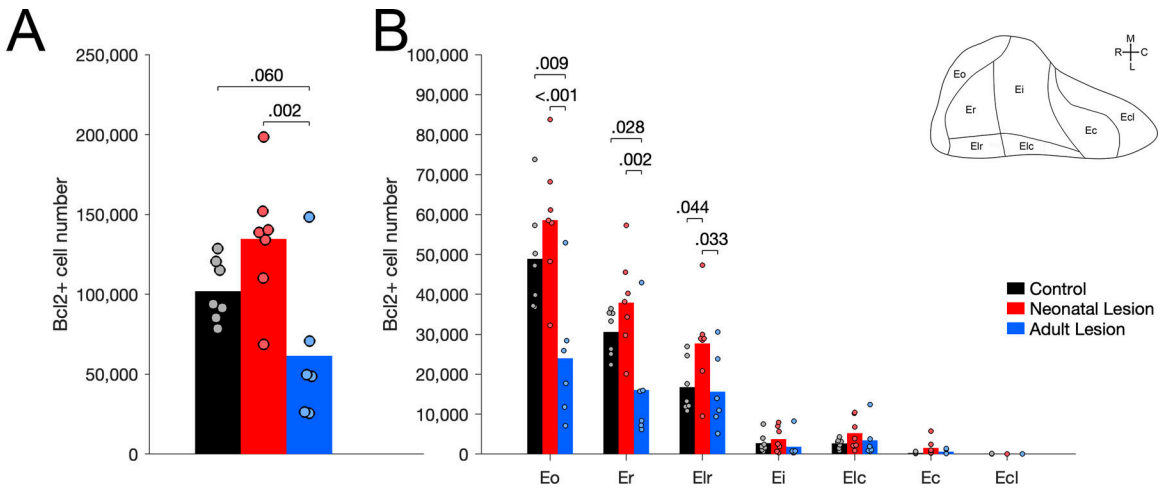

Figure 4.

Number of Bcl2+ cells in the entorhinal cortex of unoperated control (black), neonatal hippocampal-lesioned (red) and adult hippocampal-lesioned (blue) monkeys. **A.** Number of Bcl2+ cells through the entire entorhinal cortex. **B.** Number of Bcl2+ cells in the distinct subdivisions of the entorhinal cortex (Eo, Er, Elr, Ei, Elc, Ec, Ecl).

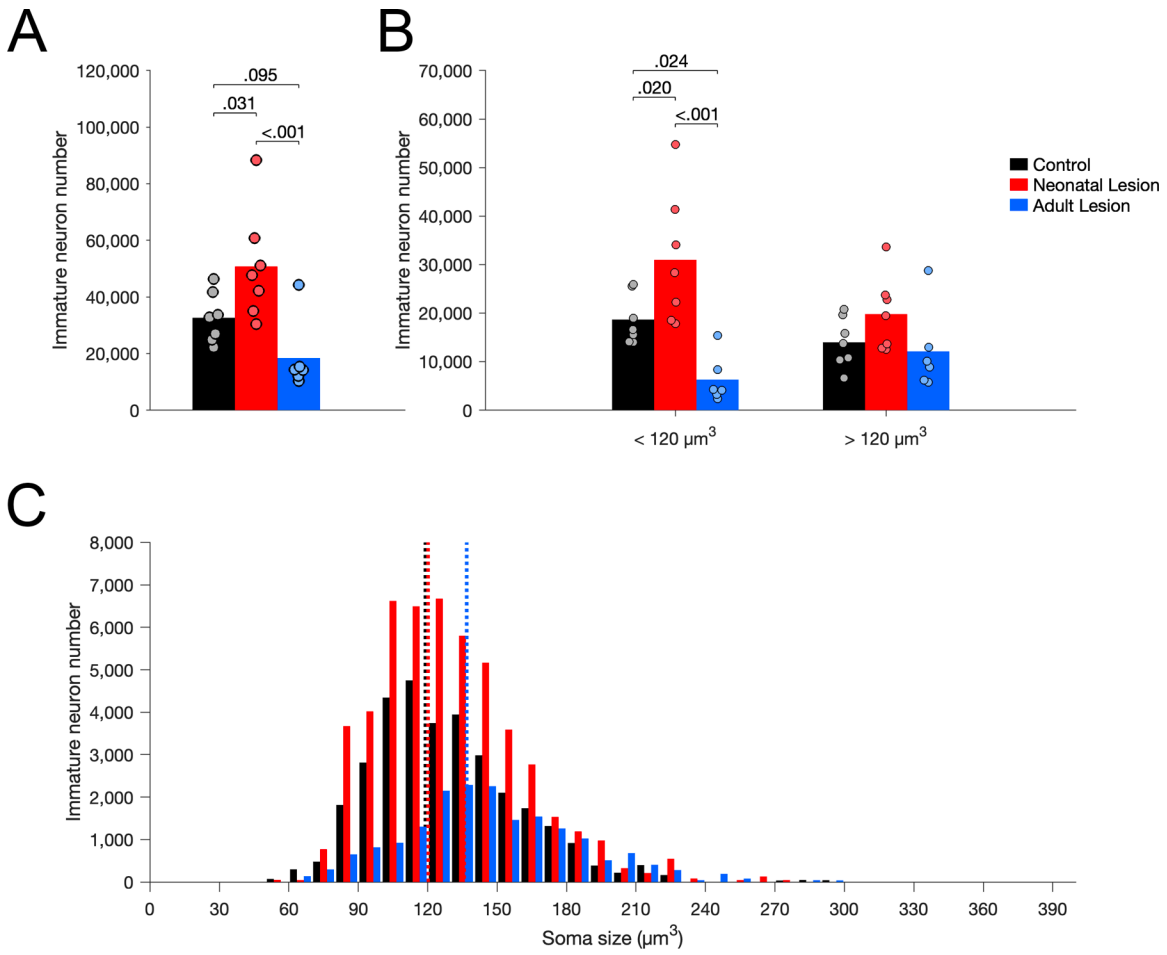

Figure 5.

Number of Nissl-stained immature neurons in layer III of area Er in unoperated control (black), neonatal hippocampal-lesioned (red) and adult hippocampal-lesioned (blue) monkeys. **A.** Total number of immature neurons. **B.** Number of small and large immature neurons, below and above the median soma size of controls (120 μm^3). **C.** Distribution of immature neuron soma size (in cubic micrometers, μm^3). Dotted lines represent the average soma size for each group (controls: 119 μm^3; neonatal lesion: 120 μm^3; adult lesion: 137 μm^3).

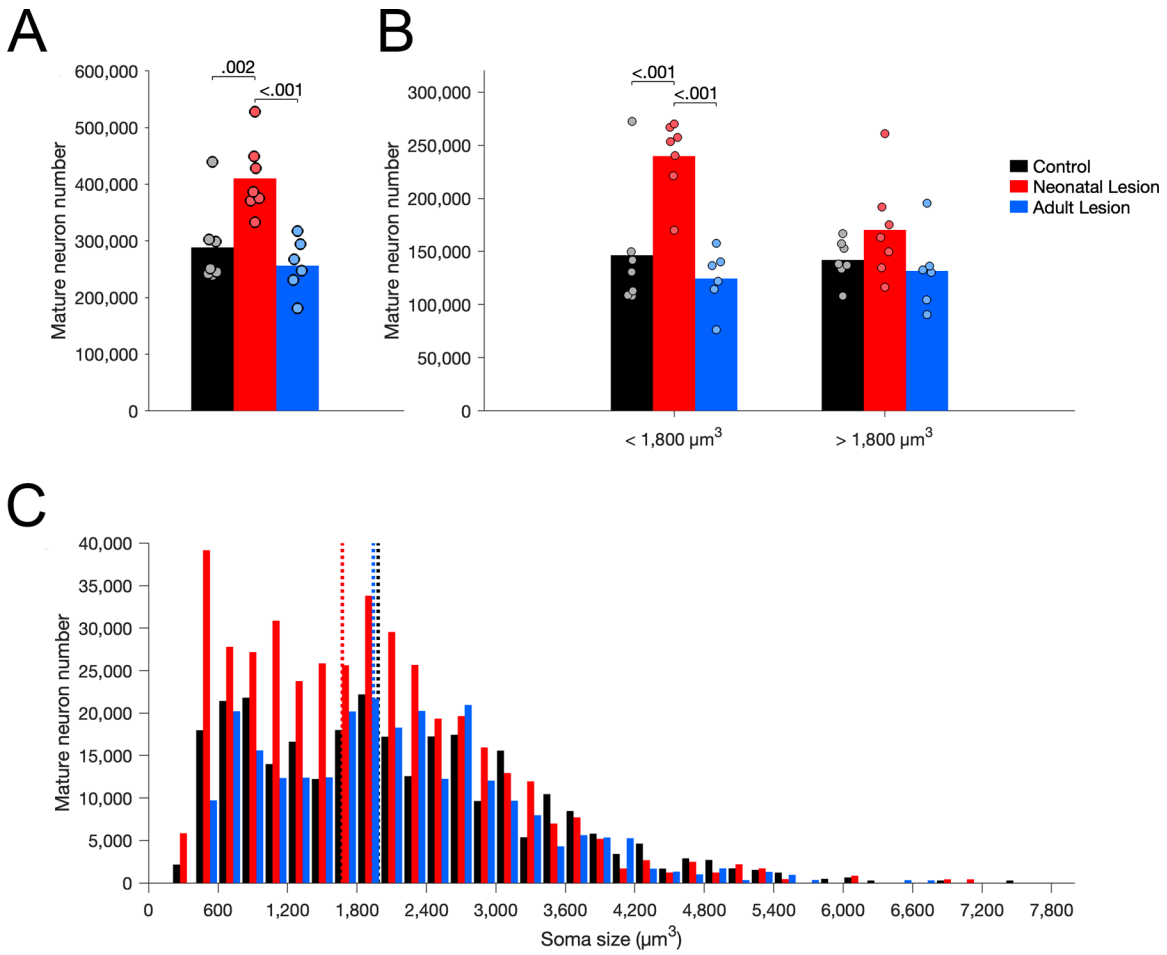

Figure 6.

Number of Nissl-stained mature neurons in layer III of area Er in unoperated control (black), neonatal hippocampal-lesioned (red) and adult hippocampal-lesioned (blue) monkeys. **A.** Total number of mature neurons. **B.** Number of small and large mature neurons, below and above the median soma size of controls (1,800 μm^3). **C.** Distribution of mature neuron soma size (in cubic micrometers, μm^3). Dotted lines represent the average soma size for each group (controls: 1,982 μm^3; neonatal lesion: 1,673 μm^3; adult lesion: 1,941 μm^3).

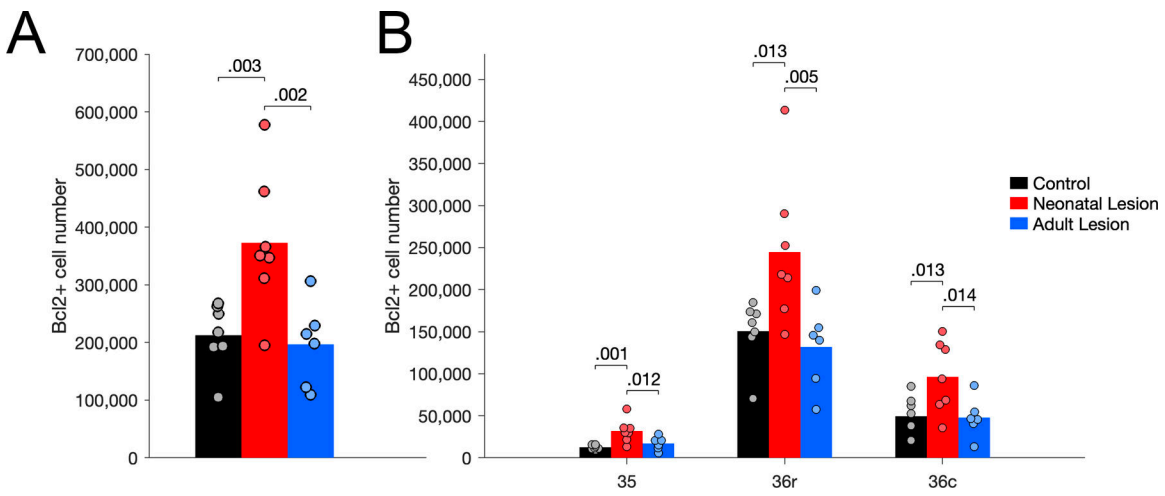

Figure 7.

Number of Bcl2+ cells in the perirhinal cortex of unoperated control (black), neonatal hippocampal-lesioned (red) and adult hippocampal-lesioned (blue) monkeys. **A.** Number of Bcl2+ cells through the entire perirhinal cortex. **B.** Number of Bcl2+ cells in the distinct subdivisions of the perirhinal cortex (areas 35, 36r, 36c).

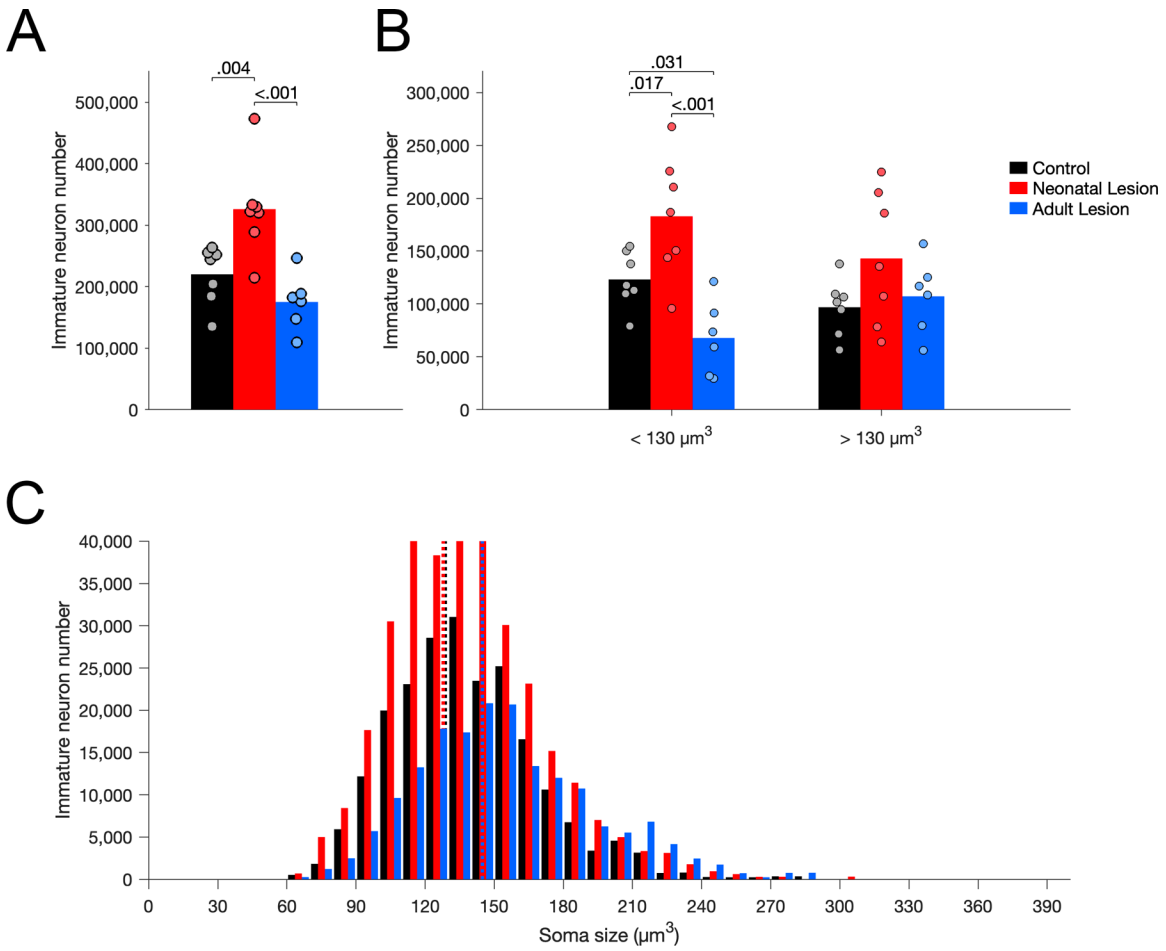

Figure 8.

Number of Nissl-stained immature neurons in layer II of area 36 in unoperated control (black), neonatal hippocampal-lesioned (red) and adult hippocampal-lesioned (blue) monkeys. **A.** Total number of immature neurons. **B.** Number of small and large immature neurons, below and above the median soma size of controls (130 μm^3). **C.** Distribution of immature neuron soma size (in cubic micrometers, μm^3). Dotted lines represent the average soma size for each group (controls: 129 μm^3; neonatal lesion: 128 μm^3; adult lesion: 145 μm^3).

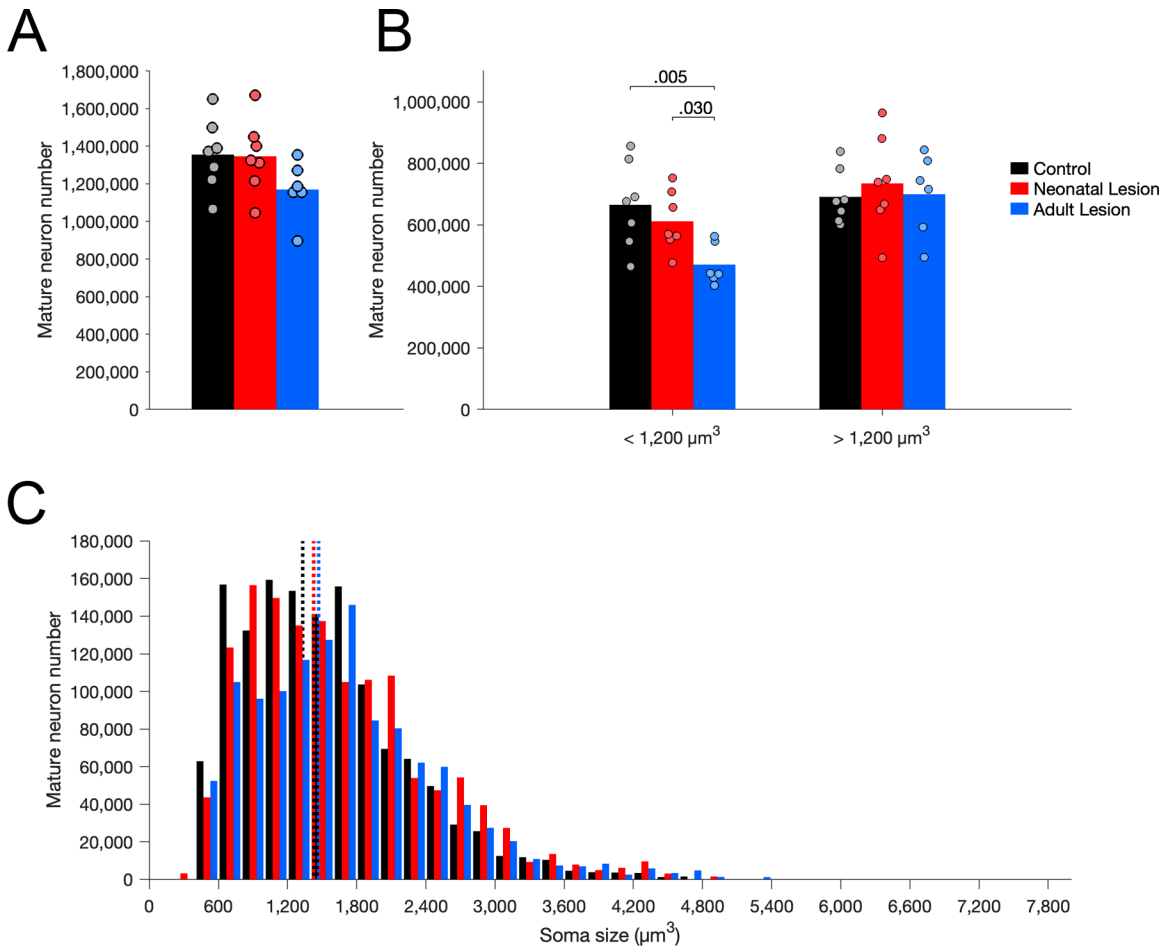

Figure 9.

Number of Nissl-stained mature neurons in layer II of area 36 in unoperated control (black), neonatal hippocampal-lesioned (red) and adult hippocampal-lesioned (blue) monkeys. **A.** Total number of mature neurons. **B.** Number of small and large mature neurons, below and above the median soma size of controls (1,200 μm^3). **C.** Distribution of mature neuron soma size (in cubic micrometers, μm^3). Dotted lines represent the average soma size for each group (controls: 1,331 μm^3; neonatal lesion: 1,426 μm^3; adult lesion: 1,469 μm^3).

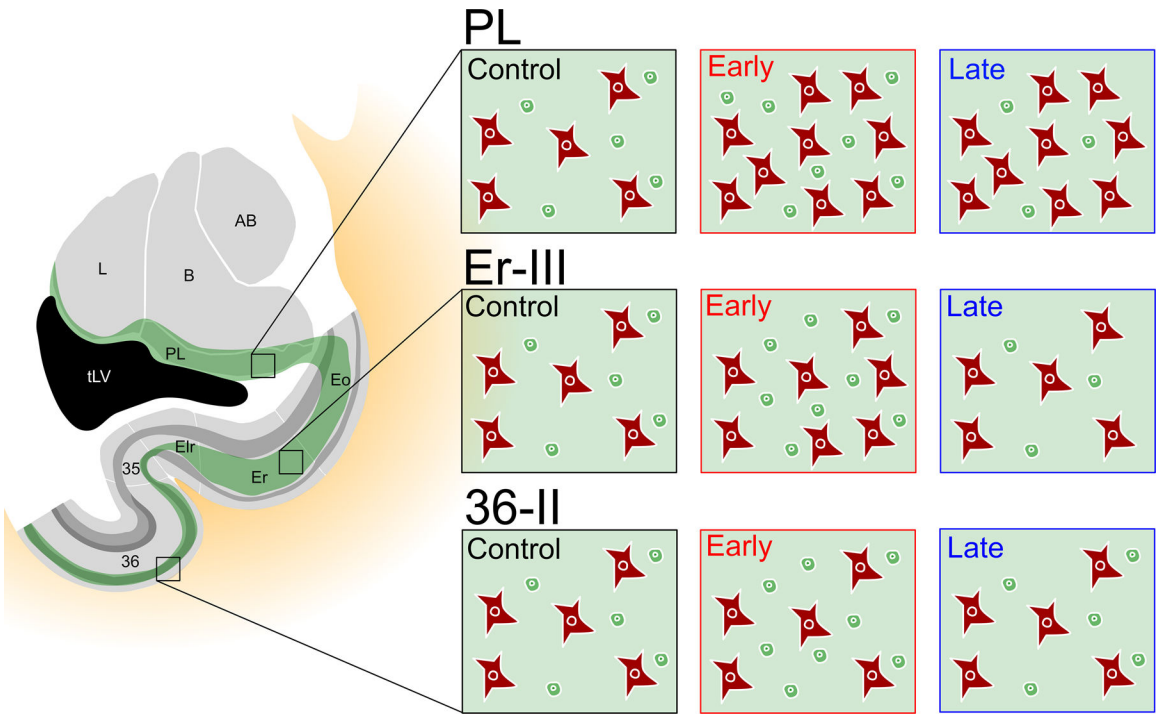

Figure 10.

Summary of the distinct changes in the number of immature and mature neurons in the paralaminar nucleus, layer III of area Er and layer II of area 36 following neonatal (Early) and adult (Late) hippocampal lesion. The changes in the number of cells reflect the percentage of change relative to the control group.